AFRL-RV-PS-
TR-2018-0101

COMMUNICATION ON THE MOVE WITH SATELLITE DIGITAL BEAMFORMING

Hyuck M. Kwon
Madkhuprana Goswami

Wichita State University
Department of Electrical Engineering and Computer Science 1845 N. Fairmount Ave.
Wichita, KS 67260-0083

14 November 2018

Final Report

APPROVED FOR PUBLIC RELEASE; DISTRIBUTION IS UNLIMITED.

AIR FORCE RESEARCH LABORATORY
Space Vehicles Directorate
3550 Aberdeen Ave SE
AIR FORCE MATERIEL COMMAND
KIRTLAND AIR FORCE BASE, NM 87117-5776

DTIC COPY

NOTICE AND SIGNATURE PAGE

Using Government drawings, specifications, or other data included in this document for any purpose other than Government procurement does not in any way obligate the U.S. Government. The fact that the Government formulated or supplied the drawings, specifications, or other data does not license the holder or any other person or corporation; or convey any rights or permission to manufacture, use, or sell any patented invention that may relate to them.

This report is the result of contracted fundamental research which is exempt from public affairs security and policy review in accordance with AFI 61-201, paragraph 2.3.5.1. This report is available to the general public, including foreign nationals. Copies may be obtained from the Defense Technical Information Center (DTIC) (http://www.dtic.mil).

AFRL-RV-PS-TR-2018-0101 HAS BEEN REVIEWED AND IS APPROVED FOR PUBLICATION IN ACCORDANCE WITH ASSIGNED DISTRIBUTION STATEMENT.

//signed//

KHANH PHAM
Program Manager

//signed//

DAVID CARDIMONA
Tech Advisor, Missile Warning & ISR
Technology Branch

//signed//

JOHN BEAUCHEMIN
Chief Engineer, Spacecraft Technology Division
Space Vehicles Directorate

This report is published in the interest of scientific and technical information exchange, and its publication does not constitute the Government's approval or disapproval of its ideas or findings.

Approved for public release; distribution is unlimited.

REPORT DOCUMENTATION PAGE

Form Approved
OMB No. 0704-0188

Public reporting burden for this collection of information is estimated to average 1 hour per response, including the time for reviewing instructions, searching existing data sources, gathering and maintaining the data needed, and completing and reviewing this collection of information. Send comments regarding this burden estimate or any other aspect of this collection of information, including suggestions for reducing this burden to Department of Defense, Washington Headquarters Services, Directorate for Information Operations and Reports (0704-0188), 1215 Jefferson Davis Highway, Suite 1204, Arlington, VA 22202-4302. Respondents should be aware that notwithstanding any other provision of law, no person shall be subject to any penalty for failing to comply with a collection of information if it does not display a currently valid OMB control number. **PLEASE DO NOT RETURN YOUR FORM TO THE ABOVE ADDRESS.**

1. REPORT DATE *(DD-MM-YYYY)*	**2. REPORT TYPE**	**3. DATES COVERED** *(From - To)*
14-11-2018	Final Report	09 Mar 2017 – 14 Nov 2018

4. TITLE AND SUBTITLE
Communication on the Move with Satellite Digital Beamforming

5a. CONTRACT NUMBER
FA9453-17-1-0020

5b. GRANT NUMBER

5c. PROGRAM ELEMENT NUMBER
62601F

6. AUTHOR(S)
Hyuck M. Kwon and Madhuprana Goswami

5d. PROJECT NUMBER
8809

5e. TASK NUMBER
PPM00028358

5f. WORK UNIT NUMBER
EF129110

7. PERFORMING ORGANIZATION NAME(S) AND ADDRESS(ES)
Wichita State University
Department of Electrical Engineering and Computer
Science 1845 N. Fairmount Ave.
Wichita, KS 67260-0083

8. PERFORMING ORGANIZATION REPORT NUMBER

9. SPONSORING / MONITORING AGENCY NAME(S) AND ADDRESS(ES)
Air Force Research Laboratory
Space Vehicles Directorate
3550 Aberdeen Ave, SE
Kirtland AFB, NM 87117-5776

10. SPONSOR/MONITOR'S ACRONYM(S)
AFRL/RVSW

11. SPONSOR/MONITOR'S REPORT NUMBER(S)
AFRL-RV-PS-TR-2018-0101

12. DISTRIBUTION / AVAILABILITY STATEMENT
Approved for public release; distribution is unlimited.

13. SUPPLEMENTARY NOTES

14. ABSTRACT
In a satellite communication system, channel coefficients from multiple-input-multiple-output (MIMO) antennas are correlated strongly because of a long propagation distance and a narrow angle spread. This is referred to as a keyhole (KH) channel, which results in a rank deficiency in the MIMO channel, and reduction of the number of simultaneously supportable multiple-access users. In addition, a high-power amplifier (HPA) in a satellite transponder distorts the transmitted signal due to its nonlinearity and memory. The aim of this report is to study a satellite beam-forming (BF) method and to investigate its signal-to-interference-plus-noise ratio (SINR) degradation due to the KH and HPA nonlinearity effects. A closed form of an optimum BF vector is not available due to the HPA nonlinearity and memory, and a BF vector with simple complexity is desirable in practice. Therefore, this report proposes for a satellite transponder to use column vectors from a discrete Fourier transform matrix as precoding BF vectors for multiple ground terminals to meet their SINR demands. Each receiver can apply maximal ratio combining post processing for further processing gain, and should feedback his SINR observation to the transponder.

15. SUBJECT TERMS
Multiple-input, multiple-output, beamforming, keyhole channel, high-power amplifier, discrete Fourier transform, maximal ratio combining

16. SECURITY CLASSIFICATION OF:			**17. LIMITATION OF ABSTRACT**	**18. NUMBER OF PAGES**	**19a. NAME OF RESPONSIBLE PERSON**
					Khanh Pham
a. REPORT	**b. ABSTRACT**	**c. THIS PAGE**			**19b. TELEPHONE NUMBER** *(include area code)*
Unclassified	Unclassified	Unclassified	SAR	46	

Standard Form 298 (Rev. 8-98)
Prescribed by ANSI Std. 239.18

(This page intentionally left blank)

Approved for public release; distribution is unlimited.

TABLE OF CONTENTS

Section **Page**

Approved for public release; distribution is unlimited.

LIST OF FIGURES

Figure **Page**

Approved for public release; distribution is unlimited.

ACKNOWLEDGMENTS

This work was supported in part by the Air Force Research Laboratory (AFRL) under Grant FA9453-17-1-0020. The views and conclusions contained herein are those of the authors and should not be interpreted as necessarily representing the official policies or endorsements, either expressed or implied, of the AFRL or the U.S. Government.

Approved for public release; distribution is unlimited.

(This page intentionally left blank)

1.0 SUMMARY

This report achieved the three objectives stated in the original proposal during the period from March 3, 2017, to August 14, 2018, by doing the following:

- Investigated satellite digital beamforming (BF) methods that can provide a user on the move.
- Proved the proposed concept through simulation.
- Evaluated the merits and disadvantages of the proposed strategy by comparing the signal-to interference-plus-noise ratio *SINR*.

2.0 INTRODUCTION

Motivation

A satellite communication (Sat-Com) system environment is quite different in many aspects from those of terrestrial and cellular wireless communication systems. For example, the current fourth-generation (4G) and future fifth-generation (5G) wireless communication systems have exploited the benefits of channel diversity and multiplexing gain that exist in nature due to the independence among channel coefficients from multiple transmit to multiple receiver, that is, multiple-input, multiple-output (MIMO), antennas. In addition, a massive MIMO antenna in a terrestrial communication system employs a large number of antenna elements at a base station (BS) to enhance the data rate. The terrestrial channel coefficients from transmit antenna elements to receive antenna elements are considered independent and identical, i.e., a favorable channel propagation condition. A massive MIMO channel matrix can be of full rank, i.e., the minimum out of the number of transmitter antenna elements N_t and that of receiver antenna elements N_r. Hence, the multiplexing gain, i.e., the number of simultaneously supportable multiple access users can be larger than 2.

However, in a Sat-Com link, even when an MIMO antenna is employed for the link from a transponder to an end ground user terminal, or vice versa, the channel coefficients are strongly correlated to each other because of the very small angle spread in the long propagation path. This is referred to as the keyhole (KH) effect. Many existing works have demonstrated degraded channels under KH effects through physical examples where transmit and receive signals are uncorrelated but have a single degree of freedom. Hence, the maximum number of simultaneously supportable users per carrier and per time slot has been two by employing a pair of two orthogonal waveforms, e.g., a pair of right-hand circular (RHC) and left-hand circular (LHC) polarization waveforms.

In addition, a Sat-Com link has a long waveform traveling distance, especially for a geostationary earth orbit (GEO) satellite. Hence, the GEO requires extreme high transmitting power (e.g., 20 dBW = 100 Watts) because it is located 36,000 km away. Thus, it is necessary to operate close to a saturation point in a high-power amplifier (HPA), thereby causing undesirable intermodulation and nonlinear impairments.

In contrast, although an HPA is employed at a cellular BS, it is not necessary for it to operate at the maximum-output power level because of the relatively short waveform traveling distance (e.g., 10 km), thereby yielding a small path loss compared to that in a 36,000-km satellite link. Hence, an HPA in a cellular BS does not distort the transmitted signal as much as the one in a Sat-Com system.

Furthermore, most existing satellite systems have employed a phased array antenna for the beamforming (BF) and a different carrier frequency from an adjacent beam. A maximum of two users can be supported at a given time per carrier by the existing satellite BF method. Each beam can support multiple users using different time division multiple access (TDMA) slots. And the waveform round trip time is about 240 ms for a 36,000-km geodistance, which is much longer than that in a terrestrial system, e.g., 67 μs for a 10-km distance.

Therefore, the motivation of this report is the following question: Can we design a Sat-Com system digital BF similar to a cellular MIMO system BF that can support more than two user-demand signals per carrier per time slot, even under a KH and HPA nonlinearity environment?

Objective

First, the aim of this report is to find the optimum BF weight (or precoding) vectors under a massive MIMO favorable channel condition as used in [1], [2], [3], but such that each user receives a signal of the same strength.

The second aim of this report is to find the BF weight vectors according to user-demand signal quality, e.g., user l may require a strong signal-to-interference-plus-noise ratio (SINR), $SINR_l$, but user k may only need a weak $SINR_k$ due to different user applications. Thus, it is not necessary to support all users with the same data rate. The weight vector is taken as an orthonormal vector. We compare our proposed model with that in [1].

Third, this report aims to analyze for the first time the BF vector degradation due to the combined effects of multiple HPAs at the transmitter and a KH channel for a MIMO system with K number of end users distributed on the ground/air. The nonlinear HPAs in our model can act as a decode-and-forward (DF) relay satellite on-board processor.

Fourth, this report will employ the column vectors in a discrete Fourier transform (DFT) matrix as satellite precoding BF vectors as done in [4] for a practical application. The size of the DFT matrix is equal to $N_t \times N_t$, where N_t is the number of transmit antenna elements. An existing phase array antenna employs a large number of antenna elements, e.g., 256. This report will determine a combination of K column vectors out of N_t number of column vectors to support K users. This is because it is difficult to find an $N_t \times 1$ optimum precoding BF vector in a closed form for each user under the HPA nonlinearity and KH effect. The column vectors of a DFT matrix

have been used as precoding BF vectors for simple implementation with minimal degradation, as in [4], but no HPA and no KH were considered. Each user receiver on the ground needs to report its received SINR to an onboard transponder processor, which will find the best DFT column vector combination for all K users that maximizes the sum of all K users' SINRs. Therefore, the main objective of this report is to find the best combination of DFT column vectors that maximizes the sum of K users' SINRs under HPA nonlinear distortion and KH channel environments. We assume that $K \leq N_t$.

Fifth, this report will find a combination of K number of DFT column BF vectors to support K user specific SINRs.

Lastly, this report will apply a maximal ratio combining (MRC) post-processing technique at the receiver side to improve the received SINR further.

Literature Survey

Digital BF or precoding has been studied for many years for terrestrial communication links but not sufficiently yet for satellite links, including both HPA and KH effects. Only a few references have been selected for the literature survey. The authors in [1] considered a full-rank massive MIMO channel (i.e., favorable channel condition) and proposed a broadcast downlink BF vector design that maximizes the SINR of the worst user in a cell. In [2], the authors introduced the massive MIMO. In [3], the authors considered two optimization problems: maximizing a jointly achievable SINR threshold under a total power constraint, and minimizing the total transmission power while satisfying the individual SINR constraints. Most massive MIMO BF studies [1-3] in the literature have assumed the full-rank channel condition, and no HPA and no KH were considered. In [4] the column vectors in a DFT matrix were used as precoding BF vectors. Recently, in [5], a generalized multicast multibeam precoding for satellite communications was presented. Again, neither HPA nor KH were considered in [4-5]. In [6], symbol-level precoding for the nonlinear multiuser multiple-input, single-output (MISO) downlink channel was presented. In [7], the authors presented the data predistortion for multicarrier satellite channels based on direct learning. In [6-7], nonlinear amplifier effects were considered but not KH. Other symbol-level precoding studies have appeared recently [8]-[10]; however, no KH was considered. Symbol-level precoding requires a full rank channel matrix, and a KH channel rank of only 1. The authors in [11] measured and studied keyhole channel effects on MIMO channel capacity, but HPA was not considered.

The high-power amplifier is an important topic of research in satellite communication, and there is considerable research on this topic. The most commonly known HPA model is that of Saleh [12]-[14]. Again, the KH effect was not considered in the literature that studied the HPA. This report will include both Saleh's HPA model and KH effects. The method in this report can be applied to other HPA models as well.

The rest of the report is organized as follows. Section 4 is subdivided into two sections. Subsection 4-A introduces a massive MIMO system model with end users having a single antenna element and without any channel degradation due to HPA nonlinearity and the KH effect. Subsection 4-B presents the MIMO system model with nonlinear HPAs and keyhole effects,

followed by a system with no KH channel and no HPA distortion, a system with only the KH channel but no HPA, and a system with no KH but only an HPA at the transmitter side. In this subsection the user has multiple antenna elements. Section 5 presents the simulation results and discussions. Section 6 draws the conclusion.

Uppercase boldface letters denote matrices, while lowercase boldface and italicized letters denote column vectors. All italicized letters denote scalar quantities. The symbols $x||,||\boldsymbol{x}||$, and x^H denote the magnitude, norm, and Hermitian operators, respectively, and $E[]X$ stands for expectation of a random variable X.

3.0 METHODS, ASSUMPTIONS, AND PROCEDURES

In this report the following five system models are studied:

A. **Massive MIMO System Channel Model: With Single Antenna at Each End User and No Channel Degradation Due to HPA and KH Effect;**

B. **MIMO System Channel Model: With Multiple Antennas at Each End User and Channel Degradation Due to HPA and KH Effect;**

C. **MIMO System Channel Model: With Multiple Antennas at Each End User and Channel Degradation Due to HPA and No KH Effect;**

D. **MIMO System Channel Model: With Multiple Antennas at Each End User and Channel Degradation Due to No HPA and KH Effect;**

E. **MIMO System Channel Model: With Multiple Antennas at Each End User and Channel Degradation Due to No HPA and No KH Effect.**

System models *A* and *E* are more valid for a terrestrial 5G wireless communications system than a satellite channel, and the other System Models *B, C,* and *D* are more reasonable and useful for a satellite channel communication system with a long propagation distance such as a GEO link than a terrestrial channel. System Models *C, D,* and *E,* are special cases of System Model *B*. Therefore, this report focuses more on System Models *A* and *B* in Theoretical Analysis Section, and presents simulation results in Results and Discussion Section for all System Models including *C, D,* and *E*.

4.0 PROCEDURE (THEORETICAL ANALYSIS)

A. Massive MIMO System Channel Model: With Single Antenna at Each End User and No Channel Degradation due to HPA and KH Effect

In this section, we propose a massive MIMO system model where each end user has a single (in this subsection model only) antenna element, and all users in a zone *i* behave as several distributed antennas together. We consider *n* satellites, and each satellite has *M* antenna elements.

In Figure 1, the angular difference between the transmitted signal and the interfering signal is 45 degrees for example. Satellite *i* is assumed to support two users in zone *i* for the simulation purpose. It may support more users as well. Satellite *j* also supports two users in zone *j*. The signal from satellite *j* interferes with the transmitted signal from satellite *i* to user *k* in zone *i*. The potential number of users (*K*) in each zone is assumed to be the same. All users may or may not utilize the service provided by the network all the time.

Figure 2 shows how the desirable data rate R_{ik} can be expressed as a function of bandwidth B_{ik}, $SINR_{ik}$, modulation, and forward error-correction coding (FEC). In order to achieve the goals that motivated this work, adaptive digital beamforming [1] is employed at satellite *i* with MIMO antenna elements to support *K* users in its zone *i*. Satellite *i* supports users in zone *i*, and $SINR_{ik}$ is dependent on user *k* in zone *i*, $k = (1, \ldots, K)$ users, $i = (1, \ldots, n)$ satellites.

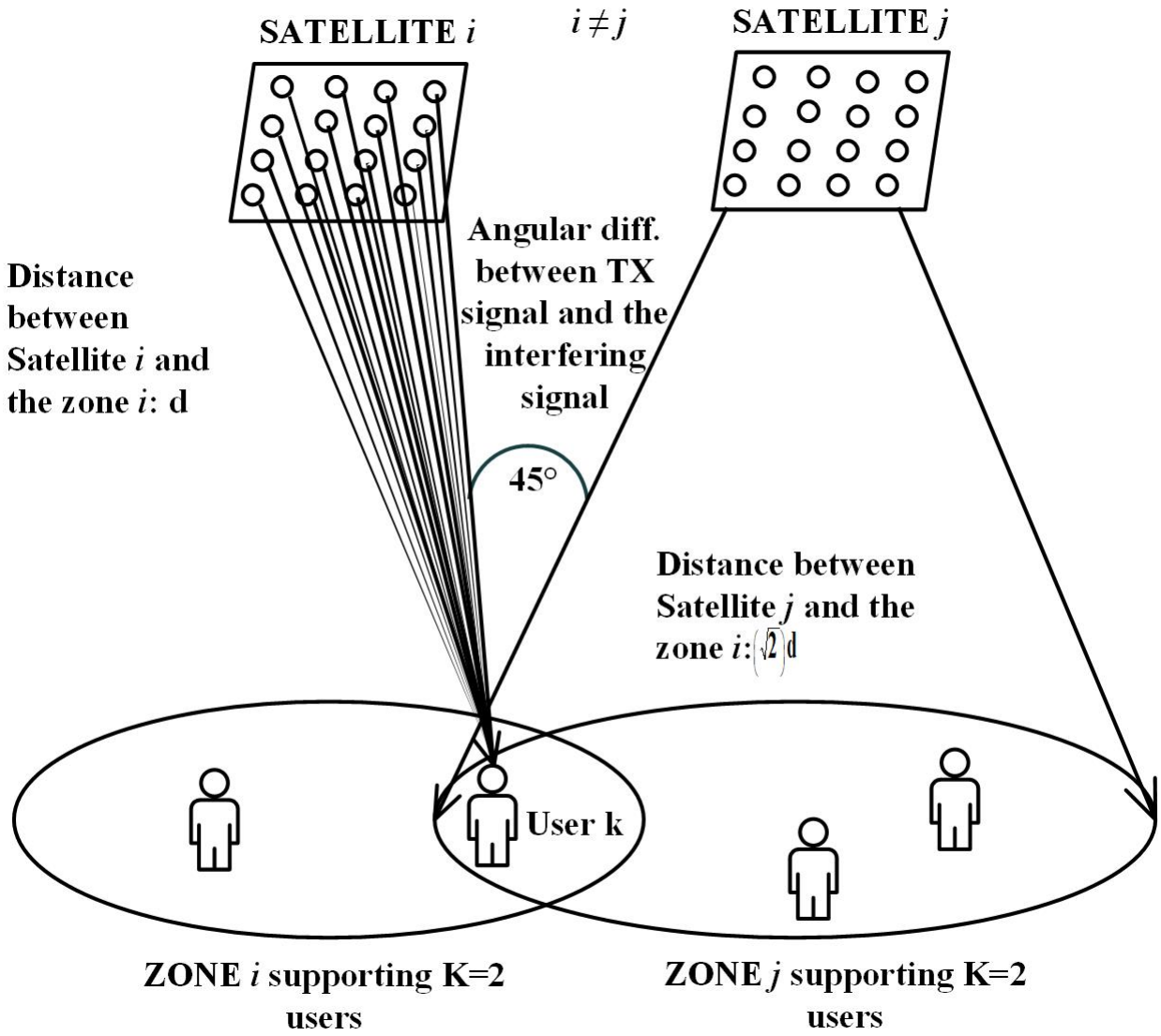

Figure 1. Satellite Digital Beamforming Considered for Simulation Results

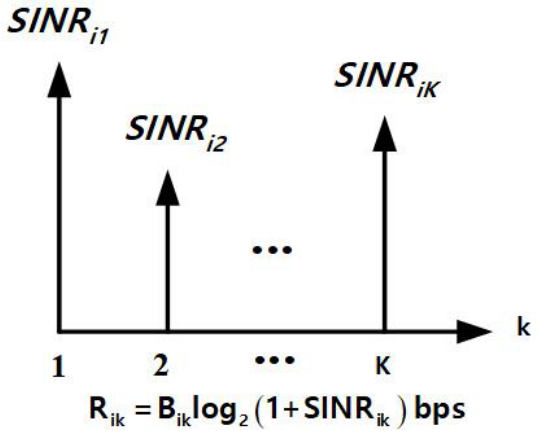

Figure 2. User-specific SINR versus User Index *k*

In Figure 3, the multicast information symbol, s_i, is a copy of the data that is multicast by satellite *i* to all *K* users in multiple zones, whereas the individual data information symbol s_{ik} for user *k* in zone *i* is the user replicated data that can be used according to the requirement of each user [1]. It should be noted that $E[|s_i|^2]$ is equal to 1.

The large-scale fading or slowly changing fading or the free space path loss gain from satellite *i* to user *k* in zone *j* can be expressed as

$$\beta_{ijk} = \left(\lambda_i \sqrt{G_{ijkT} G_{ijkR}} \Big/ d_{ik}\right)^2. \tag{1}$$

where G_{ijkT} is satellite *i*'s transmitter antenna gain in the direction of user *k* in zone *j*, G_{ijkR} is user *k*'s receiver antenna gain in zone *j* in the direction of satellite *i*, $k = 1 \text{L } K$ users, $i, j = 1 \text{L } n$ satellites, and λ_i is the wavelength. The distance between user *k* and the *i*-th and *j*-th satellites is denoted by d_{ik} and d_{jk}, respectively. The channel vector from satellite *i* to user *k* in zone *j* with a length *M* can be written as

$$\boldsymbol{g}_{ijk} = \left(\sqrt{\beta_{ijk}} h_{ijk1}, \quad \text{L}, \quad \sqrt{\beta_{ijk}} h_{ijkM}\right)^T \tag{2}$$

Where h_{ijkm} is a small-scale fading or fast-changing fading identical independent distributed Rician or Rayleigh fading coefficient due to the surrounding objects near user *k* in zone *j* from the satellite *i*'s *m*-th antenna element and $m = 1 \text{L } M$ antenna elements. Equation (2) can be further written as

$$\boldsymbol{g}_{ijk} = \left(\sqrt{\beta_{ijk}}\right) \boldsymbol{h}_{ijk}, \tag{3}$$

where

$$\boldsymbol{h}_{ijk} = \left(h_{ijk1}, \quad \text{L}, \quad h_{ijkM}\right)^T \tag{4}$$

and has a complex Gaussian normal distribution: $CN\left(0, I_M\right)$.

Figure 3 also shows a unit-norm multicasting BF vector that is used to manipulate the SINR for users based on their demand. The BF vector of length *M* can be expressed as

$$\boldsymbol{w}_i = \left(w_{i1}, \quad \text{L} \ , \quad w_{iM} \right)^T . \tag{5}$$

This section also shows how the unit-norm multicasting BF vector helps to form multiple beams steered in different directions for the adaptive BF in multidimensional vector space.

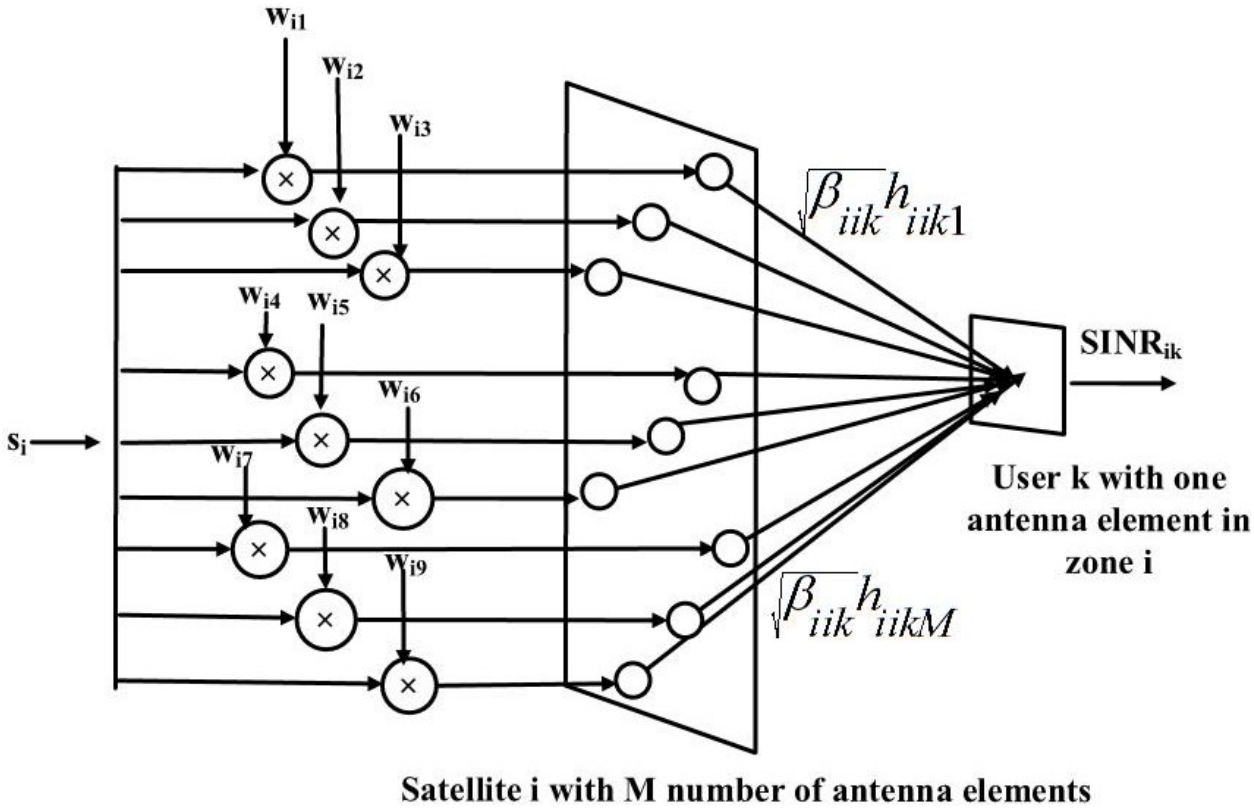

Figure 3. Satellite *i*'s Digital BF for User *k* in Zone *i* with Massive MIMO

The network considered in this subsection is a synchronized non-cooperative satellite network, i.e., satellites and users are synchronized in time and share the same frequency band, and since the network is non-cooperative, satellite *i* supports users in zone *i* only [1]. Based on the network choice the discrete-time baseband signal received by user *k* in zone *i* can be expressed as

$$\boldsymbol{x}_i = \left(\sqrt{P_i} \boldsymbol{w}_i s_i \right) \tag{6}$$

i

where satellite *i*'s transmit power is P. The discrete-time base-band signal received by user *k* in zone *i* can be expressed as

$$\boldsymbol{y}_i = \sum_{j=1}^{N} \boldsymbol{g}_{jik}^H \boldsymbol{x}_j + z_{ik}. \tag{7}$$

where z_{ik} is a complex additive white Gaussian noise (AWGN) vector with: $CN\left(0, \sigma^2\right)$ at user *k* in zone *i*, and the channel vector from satellite *j* to user *k* in zone *i*, for $j \neq i$ can be expressed as $\boldsymbol{g}_{jik}$. The received signal has two components: desirable interference, and undesirable interference with AWGN. We can further express the received signal as

$$\boldsymbol{y}_i = \sqrt{P_i}\boldsymbol{g}_{iik}^H \boldsymbol{w}_i s_i + \sum_{j \neq i}^{N} \sqrt{P_j}\boldsymbol{g}_{jik}^H \boldsymbol{w}_j s_j + z_{ik}. \tag{8}$$

where the first term is the desirable component, the second term is the undesirable interference, and z_{ik} is the AWGN with distribution $CN\left(0, \sigma^2\right)$ at user *k* in zone *i*. The SINR for the *k*-th user in the *i*-th zone can be written as

$$SINR_{ik} = \frac{E\left[\left|\sqrt{P_i}\boldsymbol{g}_{iik}^H \boldsymbol{w}_i s_i\right|^2\right]}{E\left[\left|\sum_{j \neq i}^{N} \sqrt{P_j}\boldsymbol{g}_{jik}^H \boldsymbol{w}_j s_j\right|^2\right] + E\left[\left|z_{ik}\right|^2\right]}. \tag{9}$$

Since $E[|s_i|^2]$ and $E[|s_j|^2]$ are 1, (9) can be simplified to

$$SINR_{ik} = \frac{P_i \left|\boldsymbol{g}_{iik}^H \boldsymbol{w}_i\right|^2}{\sum_{j \neq i}^{N} P_j \left|\boldsymbol{g}_{jik}^H \boldsymbol{w}_j\right|^2 + \sigma^2}. \tag{10}$$

We try to find the BF weight vectors $\boldsymbol{w}_i$ such that the SINR for all *K* users in zone *i* can be achieved based on the user requirements.

Since we consider a non-cooperative satellite network, satellite *i* supports only users in zone *i*. The first objective here is to find the weight vector $\boldsymbol{w}_i$ such that $SINR_{i1} \text{ L } SINR_{iK}$ all are constants, i.e., each user receives a signal of the same strength. The first objective function can be expressed as

$$\begin{pmatrix} SINR_{i1} \\ \text{M} \\ SINR_{iK} \end{pmatrix} = \begin{pmatrix} c \\ \text{M} \\ c \end{pmatrix} = c \begin{pmatrix} 1 \\ \text{M} \\ 1 \end{pmatrix} = c\boldsymbol{1}, \tag{11}$$

under the constraint $\|\boldsymbol{w}_i\| = 1$, i.e., the weight vector is taken to be an orthonormal vector because it helps to normalize the signal power. Also, the constant *c* is positive. Simulation results will help to understand exactly how the $SINR_{ik}$ in the first objective function has been kept constant for all users.

The second objective function finds the weight vector $\boldsymbol{w}_i$ such that $SINR_{i1}$ L $SINR_{iK}$ can be different from one another, i.e., user-specific resources can be allocated to all *K* users. The second objective function can be expressed as

$$\begin{pmatrix} SINR_{i1} \\ \mathsf{M} \\ SINR_{iK} \end{pmatrix} = \begin{pmatrix} c_1 \\ \mathsf{M} \\ c_K \end{pmatrix} @\boldsymbol{c}_i \tag{12}$$

under the same constraint $\|\boldsymbol{w}_i\| = 1$ and $c_k > 0$, where $k = 1\mathsf{L}\ K$ users. In this subsection the SINRs at the receiver are averaged over the noise samples. The optimum weight vector that satisfies the user demand vector in Equation (12) can be written as

$$\boldsymbol{w}_i^* = \alpha\left(GG^H\right)^{-1} G^H \boldsymbol{c}_i \tag{13}$$

where α is for the BF weight vector normalization and

$$G = \left(\boldsymbol{g}_{ii1}, \quad \mathsf{L}\ , \quad \boldsymbol{g}_{iiK}\right). \tag{14}$$

The proposed model in this section is compared with the referred model in [1], where the authors presented a beamforming approach for terrestrial communications simply by maximizing the SINR of the worst user receiver with single antenna element. The proposed model introduced in this subsection presents a modified transmit beamforming scheme where weight vectors are obtained so that they help to reach the target downlink SINR according to the user requirement. The authors in [1] maximized the SINR of the worst user as

$$\max_{\boldsymbol{w}_i} \min_{k\in 1,\mathsf{L}\ ,K} SINR_{ik} \quad s.t.\ \|\boldsymbol{w}_i\| = 1. \tag{15}$$

The optimum weight vector in [1] was derived as

$$\boldsymbol{w}_i^* = \mu_i \sum_{k=1}^{K} \frac{g_{iik}}{\beta_{iik}} \tag{16}$$

where

$$\mu_i = 1\Big/\sqrt{M\sum\nolimits_{k=1}^{K}\left(1/\beta_{iik}\right)}. \tag{17}$$

The simulation results in this report will support our theoretical discussion in Equations (13)-(17) more clearly.

B. MIMO System Channel Model: With Multiple Antennas at Each End User and Channel Degradation due to HPA and KH Effect

In this subsection, we obtain the BF vectors using a commonly known DFT matrix, and we consider channel degradation scenarios due to HPA and KH effects. We present the four system models and then formulate the sum of the SINRs of all users to find the optimum precoding BF vector combination. Discussion includes the differences between MRC post processing and no post processing at the receiver. All user signals use the same carrier frequency; hence, no intermodulation product will be considered. Furthermore, we find the DFT BF vectors that may help us to achieve user specific SINRs such that

$$SINR_k > SINR_{k\_Th}. \tag{18}$$

where $SINR_{k\_Th}$ is the user demand SINR threshold. Our algorithm that will be discussed later helps us to understand how SINRs of all users simultaneously satisfy the condition as expressed in Equation (18).

B-1. MIMO System Channel Model: With HPAs and Keyhole Effect

We consider an MIMO system with N_t transmit antennas and N_r receiver antennas. In our model, as shown in Figure 1, user k 's symbol s_k is transmitted to *K* receivers on the ground/air, but it is intended to be delivered to user k. The HPAs in Figure 4 can represent an on-board satellite decode-and-forward (DF) transponder of multiple transmit antenna elements for a downlink. Saleh's nonlinear HPA model [12]-[14] is considered in this report. The proposed method selects a BF vector $\boldsymbol{w}_k$ from the BF codebook and constructs it using an $(N_r \times N_t)$ DFT matrix:

$$\boldsymbol{W}_{DFT} = \left[\boldsymbol{w}_{DFT,1} \quad \mathsf{L} \quad \boldsymbol{w}_{DFT,N_t} \right] = \frac{1}{\sqrt{N_t}} \begin{bmatrix} e^{-j2\pi \cdot 0 \cdot 0/N_t} & \mathsf{L} & e^{-j2\pi \cdot 0 \cdot (N_t-1)/N_t} \\ \mathsf{M} & \mathsf{O} & \mathsf{M} \\ e^{-j2\pi \cdot (N_t-1) \cdot 0/N_t} & \mathsf{L} & e^{-j2\pi \cdot (N_t-1) \cdot (N_t-1)/N_t} \end{bmatrix}. \tag{19}$$

where $\boldsymbol{w}_{DFT,k}$ is an $N_t \times 1$ column vector employed for a distributed user k on the ground/air, $k \in \{1 \cdots K\}$. Because there are N_t number of column vectors in $\boldsymbol{W}_{DFT}$, we can choose K number of BF vectors out of N_t number of possible column vectors because one orthonormal weight vector is necessary for each user. The transmit antenna elements as modelled in Figure 4 use the same transmitting power. There are $(N_t)!/\{(K!)(N_t - K)!\}$ number of combinations. The dimension of each BF vector is $N_t \times 1$.

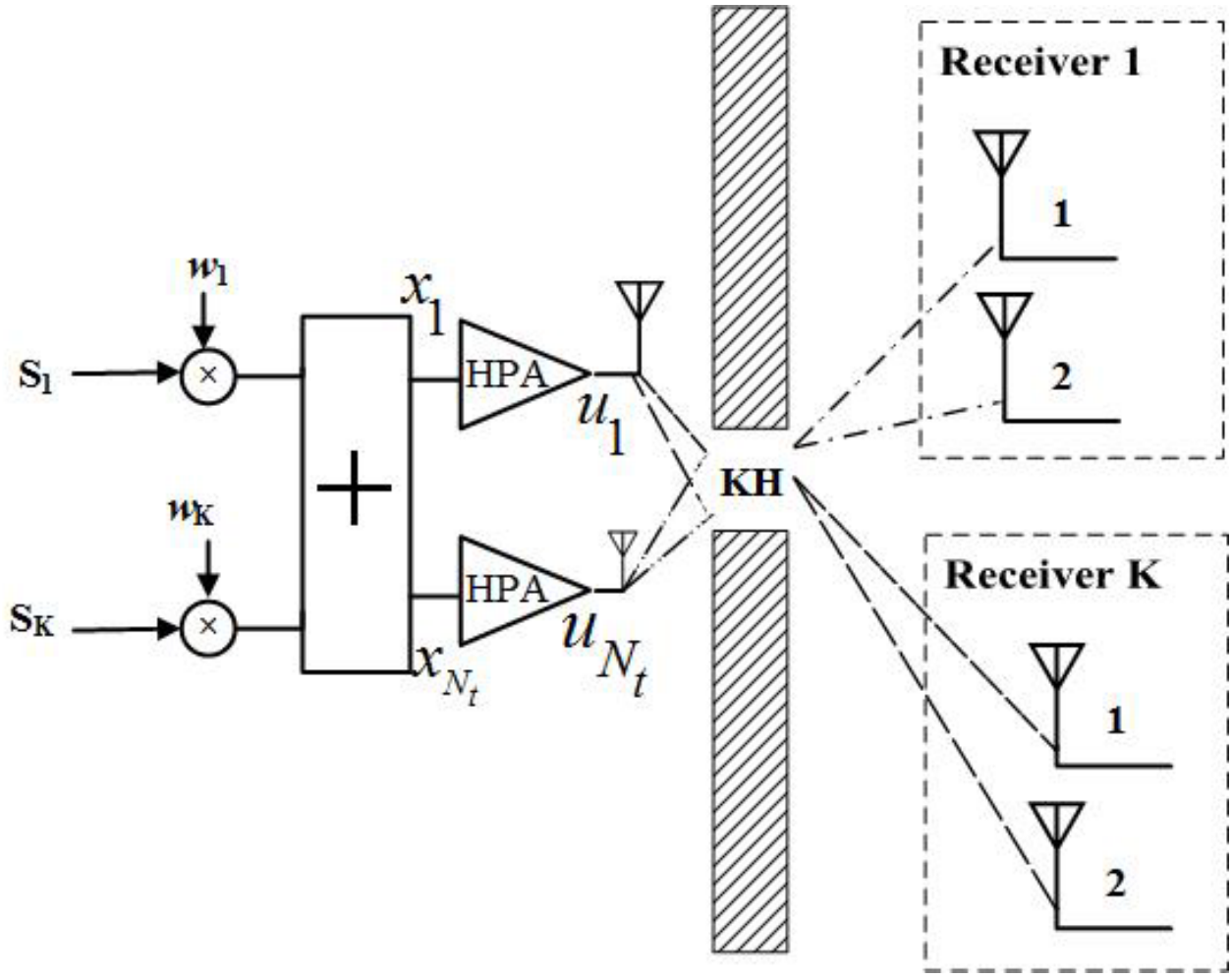

Figure 4. MIMO System Channel Model with HPA and KH

The selected BF vector $\boldsymbol{w}_k$ is multiplied to the *k*-th user modulated symbol, which is to be transmitted by the DF transponder to the users on the ground/air. The vector sum signal $\boldsymbol{x}$ will be input to a satellite transponder consisting of N_t number of HPAs. The received signal vector $\boldsymbol{y}_k$ with a dimension of $N_r \times 1$ at the *k*-th receiver (which has N_r number of receive antenna elements) is written as

$$\boldsymbol{y}_{k,DFT} = \mathbf{H}_{KH}^{k}\left(\boldsymbol{v} \circ \boldsymbol{W}\, \boldsymbol{s}\right) + \boldsymbol{n}_k . \tag{20}$$

where "$\circ$" denotes the component-by-component product called Hadamard product, and $\mathbf{H}_{KH}^{k}$ denotes the keyhole channel matrix of dimension $N_r \times N_t$ with a rank 1 for the *k*-th user and can be expressed as

$$\mathbf{H}_{KH}^{k} = \boldsymbol{h}_{N_r}^{k} \boldsymbol{h}_{N_t}^{k} = \begin{bmatrix} h_{k1} h_{k1} & \mathsf{L} & h_{k1} h_{kN_t} \\ \mathsf{M} & \mathsf{O} & \mathsf{M} \\ h_{kN_r} h_{k1} & \mathsf{L} & h_{kN_r} h_{kN_t} \end{bmatrix}. \tag{21}$$

The channel coefficient column vector for user *k* at the receiver, denoted by $\boldsymbol{h}_{N_r}^{k}$ of dimension $N_r \times 1$, is a circular symmetric complex Gaussian column vector in nature. Similarly, the channel coefficient row vector for user *k* at the transmitter, denoted by $\boldsymbol{h}_{N_t}^{k}$ of dimension $1 \times N_t$, is also circular symmetric complex Gaussian in nature. The AWGN is denoted by vector $\boldsymbol{n}_k$ in Equation (20) of $N_r \times 1$ dimension, and it has zero mean and a covariance matrix $E\left[\boldsymbol{n}_k \boldsymbol{n}_k^H\right] = N_0 I_{N_r}$. In Equation (20), the $N_r \times K$ BF matrix $\boldsymbol{W}$ is chosen from the BF codebook in Equation (19), and can be expressed as

$$\boldsymbol{W} = \left[\boldsymbol{w}_1 \quad \mathsf{L} \quad \boldsymbol{w}_K\right]. \tag{22}$$

The amplitude-to-amplitude (AM/AM) and amplitude-to-phase (AM/PM) characteristics of the memoryless HPA are denoted by

$$\underset{(N_t \times 1)}{\boldsymbol{v}} = \frac{f_A\left(|\boldsymbol{x}|\right)}{|\boldsymbol{x}|} e^{j f_P(|\boldsymbol{x}|)}. \tag{23}$$

The amplitude deviation based on AM/AM characteristics and the phase deviation based on AM/PM characteristics are expressed, respectively, as

$$f_A\left(|\boldsymbol{x}|\right) = \frac{\alpha_A |\boldsymbol{x}|}{1 + \beta_A |\boldsymbol{x}|^2} \tag{24}$$

and

$$f_P\left(|\boldsymbol{x}|\right) = \frac{\alpha_P |\boldsymbol{x}|^2}{1 + \beta_P |\boldsymbol{x}|^2}. \tag{25}$$

According to Saleh's nonlinear HPA model in [12], $\left(\alpha_A = 2, \beta_A = 1\right)$ and $\left(\alpha_P = 4, \beta_P = 9.1\right)$. In Equation (24), $\boldsymbol{x}$ is the input vector to the HPAs with dimension $N_t \times 1$ and is expressed as

$$\underset{(N_t \times 1)}{\boldsymbol{x}} = \begin{pmatrix} x_1 \\ \mathsf{M} \\ x_{N_t} \end{pmatrix} = \underset{(N_t \times K)}{\boldsymbol{W}} \underset{(K \times 1)}{\boldsymbol{s}}. \tag{26}$$

The $N_t \times 1$ output vector of the HPAs can be written as

$$\boldsymbol{u} = \begin{pmatrix} u_1 \\ \mathsf{M} \\ u_{N_t} \end{pmatrix} = \begin{pmatrix} v_1 \\ \mathsf{M} \\ v_{N_t} \end{pmatrix} \mathsf{o} \begin{pmatrix} x_1 \\ \mathsf{M} \\ x_{N_t} \end{pmatrix}. \tag{27}$$

When MRC post processing has not been applied, we formulate the $SINR_k$ for user *k* as

$$SINR_{k,DFT} = \frac{E\left[\left\|\left(\mathbf{H}_{KH}^{k}\left(\boldsymbol{v}\,\mathsf{o}\,\boldsymbol{w}_k\right)s_k\right)\right\|^2\right]}{N_0 + \sum_{j=1, j\neq k}^{K} E\left[\left\|\left(\mathbf{H}_{KH}^{k}\left(\boldsymbol{v}\,\mathsf{o}\,\boldsymbol{w}_j\right)s_j\right)\right\|^2\right]}. \tag{28}$$

The summed SINRs can be maximized with respect to the optimum BF vector combination as

$$\max_{(\boldsymbol{w}_l, \boldsymbol{w}_m)} \sum_{k=1}^{K=2} SINR_{k,DFT}\ . \tag{29}$$

In Equation (29), the best combination of weight vectors $(\boldsymbol{w}_l, \boldsymbol{w}_m)$ is sought for $K = 2$ users that maximizes the summed SINRs, $l \neq m$, and $l, m = 1\mathsf{L}\ N_t$. The best pair of weight vectors $(\boldsymbol{w}_l, \boldsymbol{w}_m)$ is chosen out of $\begin{pmatrix} N_t \\ K \end{pmatrix}$ number of combinations.

When MRC post processing is applied at the receiver, the received signal vector can be expressed using Equation (20) as

$$\boldsymbol{y}_{k,MRC} = \left(\mathbf{H}_{KH}^{k}\left(\boldsymbol{v}\,\mathsf{o}\,\boldsymbol{w}_k\right)\right)^H \boldsymbol{y}_{k,DFT}\ . \tag{30}$$

Then,

$$SINR_{k,MRC} = \frac{E\left[\left\|\left(\mathbf{H}_{KH}^{k}\left(\boldsymbol{v}\,\mathsf{o}\,\boldsymbol{w}_k\right)\right)^H\left(\mathbf{H}_{KH}^{k}\left(\boldsymbol{v}\,\mathsf{o}\,\boldsymbol{w}_k\right)s_k\right)\right\|^2\right]}{\left\{E\left[\left\|\left(\mathbf{H}_{KH}^{k}\left(\boldsymbol{v}\,\mathsf{o}\,\boldsymbol{w}_k\right)\right)^H \boldsymbol{n}_k\right\|^2\right] + \sum_{j=1, j\neq k}^{K} E\left[\left\|\left(\mathbf{H}_{KH}^{k}\left(\boldsymbol{v}\,\mathsf{o}\,\boldsymbol{w}_k\right)\right)^H\left(\mathbf{H}_{KH}^{k}\left(\boldsymbol{v}\,\mathsf{o}\,\boldsymbol{w}_j\right)s_j\right)\right\|^2\right]\right\}} \tag{31}$$

Similarly, we find the best BF vector pair that maximizes the sum SINR of all users as

$$\max_{(\boldsymbol{w}_l, \boldsymbol{w}_m)} \sum_{k=1}^{K=2} SINR_{k,MRC}\ . \tag{32}$$

Equations (29) and (32) are expressions for two users but can be extended for a general case of $K > 2$ users with no difficulty.

Once we obtain the individual SINRs from Equations (28) and (31), the onboard transponder checks if they are simultaneously greater than the SINR thresholds. Our objective in this case can be expressed in Equations (33) and (34). Find for all users

$$\boldsymbol{w}_l^*, \boldsymbol{w}_m^* \text{ s.t. } SINR_{k,DFT} > SINR_{k\_Th} \tag{33}$$

and

$$\boldsymbol{w}_l^*, \boldsymbol{w}_m^* \text{ s.t. } SINR_{k,MRC} > SINR_{k\_Th}\,. \tag{34}$$

The onboard transponder checks to see if our objectives are met or not through the algorithm shown in Table I. In Equations (33) and (34), $SINR_{k\_Th}$ is the threshold SINR demanded by the user. For our simulation, we assume that the SINR threshold for user 1 is 3 dB and user 2 is 5 dB, when $K = 2$ users are considered. This is further extended to $K = 3$ users.

Table 1. A Simple Search Algorithm to Find Optimum Weight Vectors that Achieve User Demand SINRs

Step	***Descriptions***
1	Find all weight vector pairs $(\boldsymbol{w}_l^*, \boldsymbol{w}_m^*)$ that satisfy the condition $SINR_{k,DFT} > SINR_{k\_Th}$, $k = 1 \text{L } K$.
2	Use the combination that generates the highest sum of SINRs.
3	Repeat Steps 1 and 2 for the MRC case.

MIMO System Channel Model: No Nonlinear HPAs and No Keyhole Effect

Here we consider an MIMO system model for no HPAs and no keyhole channels. The $SINR_{k,DFT}$ for the *k*-th user can be expressed as

$$SINR_{k,DFT} = \frac{E\left[\left\|\left(\mathbf{H}_k \boldsymbol{w}_k s_K\right)\right\|^2\right]}{N_0 + \sum_{j=1, j\neq k}^{K} E\left[\left\|\left(\mathbf{H}_k \boldsymbol{w}_j s_j\right)\right\|^2\right]} \tag{35}$$

and the $SINR_{k,MRC}$ for the *k*-th user can be expressed as

$$SINR_{k,MRC} = \frac{E\left[\left\|\left(\mathbf{H}_k \boldsymbol{w}_k\right)^H \left(\mathbf{H}_k \boldsymbol{w}_k s_k\right)\right\|^2\right]}{E\left[\left\|\left(\mathbf{H}_k \boldsymbol{w}_k\right)^H \boldsymbol{n}_k\right\|^2\right] + \sum_{j=1, j\neq k}^{K} E\left[\left\|\left(\mathbf{H}_k \boldsymbol{w}_k\right)^H \left(\mathbf{H}_k \boldsymbol{w}_j s_j\right)\right\|^2\right]} \tag{36}$$

In Equations (35) and (36), $\mathbf{H}_k$ denotes the channel coefficient matrix of dimension $N_r \times N_t$, which can be expressed as

$$\underset{(N_r \times N_t)}{\mathbf{H}_k} = \begin{pmatrix} \boldsymbol{h}_{1k} \\ \mathsf{M} \\ \boldsymbol{h}_{N_r k} \end{pmatrix} \tag{37}$$

where $\boldsymbol{h}_{1k}$ L $\boldsymbol{h}_{N_r k}$ are circular symmetric complex Gaussian row vectors of size $1 \times N_t$, where each component has zero mean and unit variance. Similar to Equations (29) and (32), we find the best BF vector combination that maximizes sum $SINR_{k,DFT}$ and sum $SINR_{k,MRC}$ for *K* users. We also apply the same algorithm as expressed previously in Table I to find if the user specific SINR demands are satisfied.

MIMO System Channel Model: With Nonlinear HPAs and No Keyhole Effect

Here, we study only the nonlinearity effect on the system due to HPAs. The KH channels are not included. The $SINR_{k,DFT}$ for the *k*-th user can be expressed as

$$SINR_{k,DFT} = \frac{E\left[\left\|\left(\mathbf{H}_k \left(\boldsymbol{v} \circ \boldsymbol{w}_k\right) s_k\right)\right\|^2\right]}{N_0 + \sum_{j=1, j\neq k}^{K} E\left[\left\|\left(\mathbf{H}_k \left(\boldsymbol{v} \circ \boldsymbol{w}_j\right) s_j\right)\right\|^2\right]} \tag{38}$$

while $SINR_{k,MRC}$ for the *k*-th user can be expressed as

$$SINR_{k,MRC} = \frac{E\left[\left\|\left(\mathbf{H}_k \left(\boldsymbol{v} \circ \boldsymbol{w}_k\right)\right)^H \left(\mathbf{H}_k \left(\boldsymbol{v} \circ \boldsymbol{w}_k\right) s_k\right)\right\|^2\right]}{E\left[\left\|\left(\mathbf{H}_k \left(\boldsymbol{v} \circ \boldsymbol{w}_k\right)\right)^H \boldsymbol{n}_k\right\|^2\right] + + \sum_{j=1, j\neq k}^{K} E\left[\left\|\left(\mathbf{H}_k \left(\boldsymbol{v} \circ \boldsymbol{w}_k\right)\right)^H \left(\mathbf{H}_k \left(\boldsymbol{v} \circ \boldsymbol{w}_j\right) s_j\right)\right\|^2\right]}. \tag{39}$$

We repeat the process of finding the best weight vector combination that maximizes the sum of $SINR_{k,DFT}$ as expressed in Equation (38) for *K* users and the sum of $SINR_{k,MRC}$ as expressed in Equation (39) for *K* users.

MIMO System Channel Model: No HPAs and with Keyhole Effect

Last, we focus on MIMO channel degradation solely due to KH effects. Figure 5 shows the system model for this setup. The $SINR_{k,DFT}$ and $SINR_{k,MRC}$ expressions are expressed, respectively, as

$$SINR_{k,DFT} = \frac{E\left[\left\|\left(\mathbf{H}_{KH}^{k}\boldsymbol{w}_k s_k\right)\right\|^2\right]}{N_0 + \sum_{j=1,\, j\neq k}^{K} E\left[\left\|\left(\mathbf{H}_{KH}^{k}\boldsymbol{w}_j s_j\right)\right\|^2\right]} \tag{40}$$

and

$$SINR_{k,MRC} = \frac{E\left[\left\|\left(\mathbf{H}_{KH}^{k}\boldsymbol{w}_k\right)^H\left(\mathbf{H}_{KH}^{k}\boldsymbol{w}_k s_k\right)\right\|^2\right]}{E\left[\left\|\left(\mathbf{H}_{KH}^{k}\boldsymbol{w}_k\right)^H\boldsymbol{n}_k\right\|^2\right] + \sum_{j=1,\, j\neq k}^{K} E\left[\left\|\left(\mathbf{H}_{KH}^{k}\boldsymbol{w}_k\right)^H\left(\mathbf{H}_{KH}^{k}\boldsymbol{w}_j s_j\right)\right\|^2\right]}. \tag{41}$$

The sum of $SINR_{k,DFT}$ and the sum of $SINR_{k,MRC}$ are maximized by choosing the best BF vector combination $(\boldsymbol{w}_l, \boldsymbol{w}_m)$, as shown previously in Equations (29) and (32).

For all the above cases, each user receiver can measure $SINR_{k,DFT}$ in practice without channel matrix H_k or H_{KH}^{k} information, and report this $SINR_{k,DFT}$ from a terminal to an onboard transponder via a return link, and the on-board processor can search the optimum weight vector combination that maximizes the sum of $SINR_{k,DFT}$ in Equation (29). The weight vector combination that also achieves individual user demand SINRs can be obtained using the algorithm in Table 1.

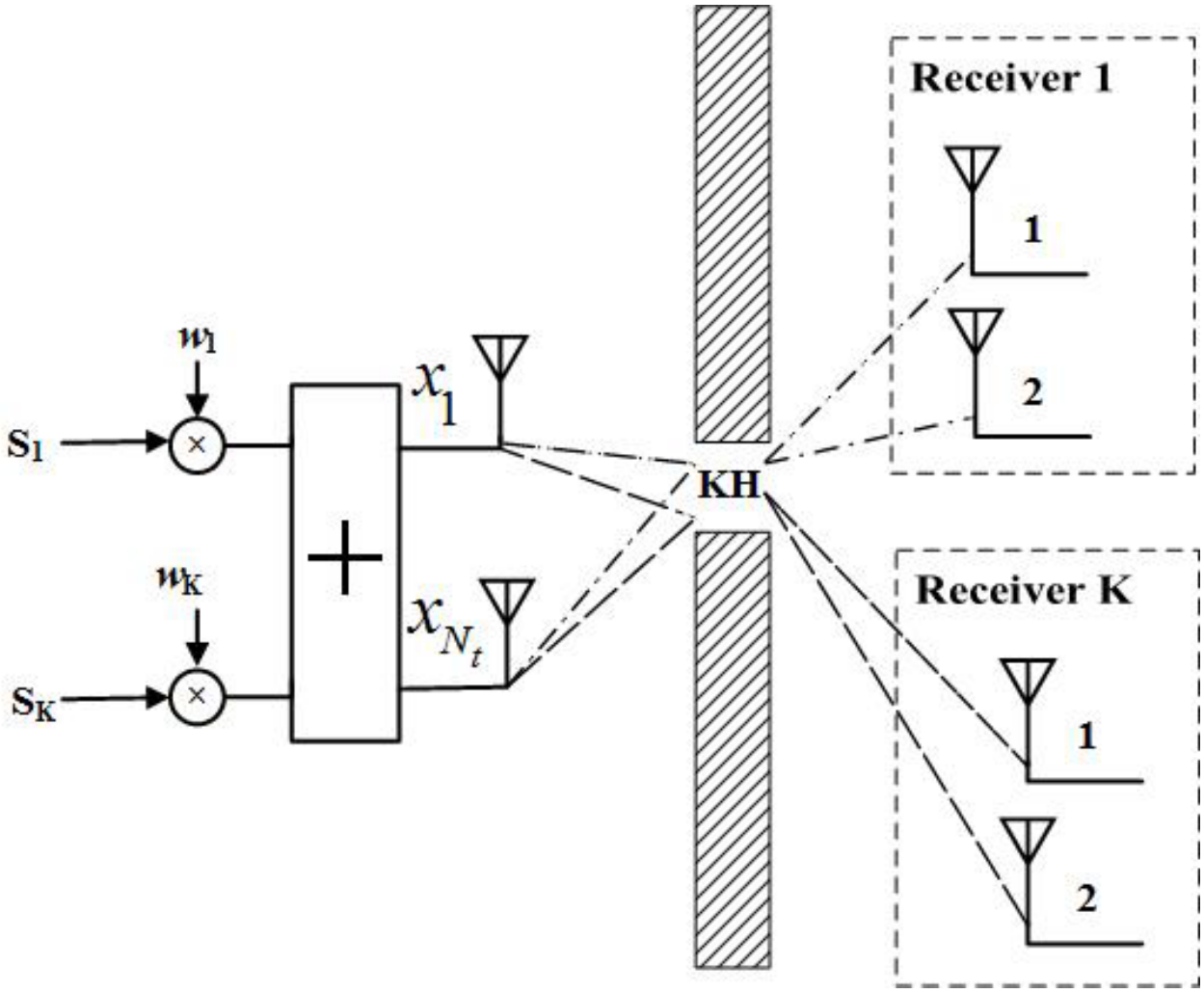

Figure 5. MIMO System Channel Model with No HPA and with KH

5.0 RESULTS AND DISCUSSION

A. Simulation for Massive MIMO System Model with Channel Degradation due to No HPA and No KH Effect, for End User Having Multiple Antenna Elements

In this subsection, our results clearly support our proposed method to find the BF vectors that achieve two objectives in Equations (11) and (12). We assume K = 2 users for the purpose of simulation. We also take the AWGN power as –204 dB, carrier frequency as 2.4 GHz, interference power P_j as –9 dB, transmit power P_i as –5 dB, distance d_{iik} from satellite i to user k in zone i as 20,000 miles, distance d_{ijk} from satellite i to user k in zone j as $\sqrt{2} \times 20,000$ miles, target SINR for objective 1 in Equation (11) as 10 dB, and target SINRs for objective 2 in Equation (12) as 10 and 50 dB. Figure 6 shows that objective 1 is satisfied, i.e., the SINR requirement by each user is 10 dB.

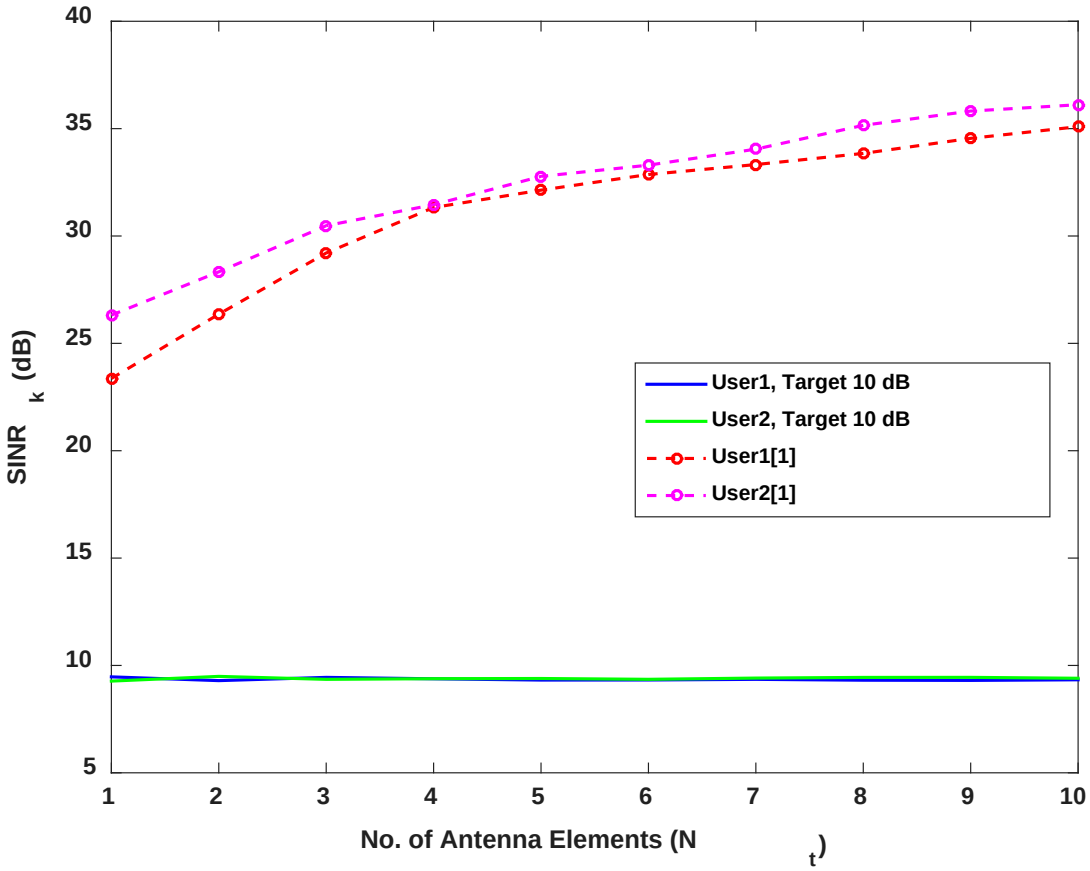

Figure 6. Comparison between Proposed Objective 1 and [1]

Figure 7 shows that objective 2 is satisfied, where the SINR requirement by user 1 is 10 dB and user 2 is 50 dB. These results help to establish the basic concept for the modified transmit BF approach for satellite communications. Throughout this subsection the channel is assumed to be perfect. It should also be noted that if interference I_{jk} due to the signal from satellite *j* interfering with the transmitted signal from satellite *i* for user *k* in zone *i*, is zero, then the $SINR_{ik}$ for each user is almost the same as that of the target SINR. When the interference I_{jk} is calculated using BF vector $\boldsymbol{w}_j$ from the *j*-th satellite to user *k* in zone *i*, the $SINR_{ik}$ for each user can be reduced by approximately 1.5 dB below the target SINR.

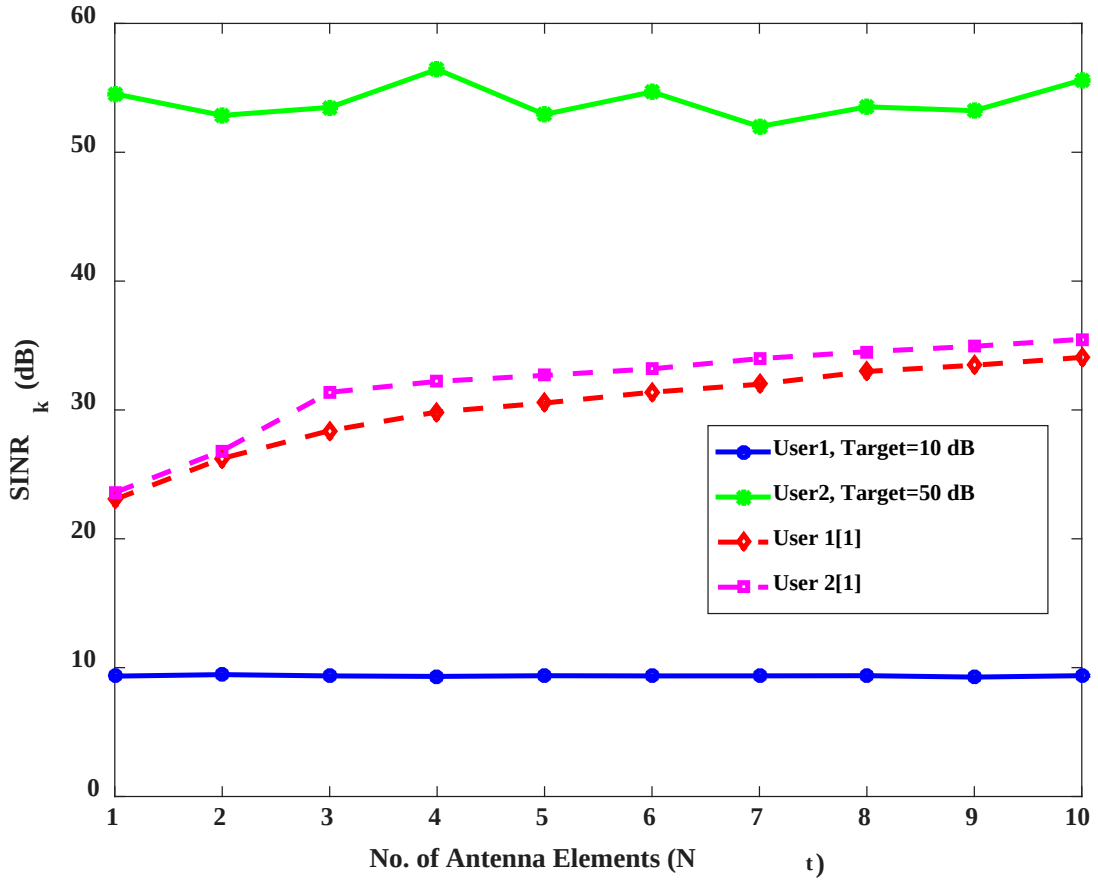

Figure 7. Comparison between Proposed Objective 2 and [1]

B. Simulation for MIMO System Model with Channel Degradation Due to HPA and KH Effect, for End User Having Multiple Antenna Elements

In this subsection, we discuss simulation results aimed at illustrating the mathematical formulation introduced earlier. For purposes of our simulation, we vary $N_t = 1 \cdots 10$ transmit antennas, $N_r = 2$ receiver antennas, $K = 2$ or 3 users, and the one-sided AWGN noise power spectral density $N_0 = 1/2$. This section is subdivided into two parts. The first part discusses simulation results with no MRC post processing, while the second part discusses simulation results with MRC post processing. Throughout our simulations we average the SINRs over 100 samples of channel coefficient matrices. The total power *P* is kept the same at 20 dB for all users, and the power at each of the N_t transmit antennas is assumed to be P / N_t.

No MRC Post Processing

Theoretically, when MRC post processing is applied at the receiver, it enhances the SINR and recovers the transmitted signal more correctly. First, we present our results for the four system models, as considered in Section II, when no post processing is present.

The MIMO system channel model with no KH channels and no HPAs shows the best performance. The sum of $SINR_{k,DFT}$ for this setup is approximately 1–2 dB higher than the sum of $SINR_{k,DFT}$ when we consider the MIMO system channel model with HPAs and no KH channels, as shown in Figure 8. The HPA output is normalized to have unit power. If the input to the HPA is close to saturation, then the output will be distorted and the SINR will be degraded. Hence, the SINR will be degraded, and the encircling denoted by *X* in Figure 8 clearly supports this observation, when $K = 2$.

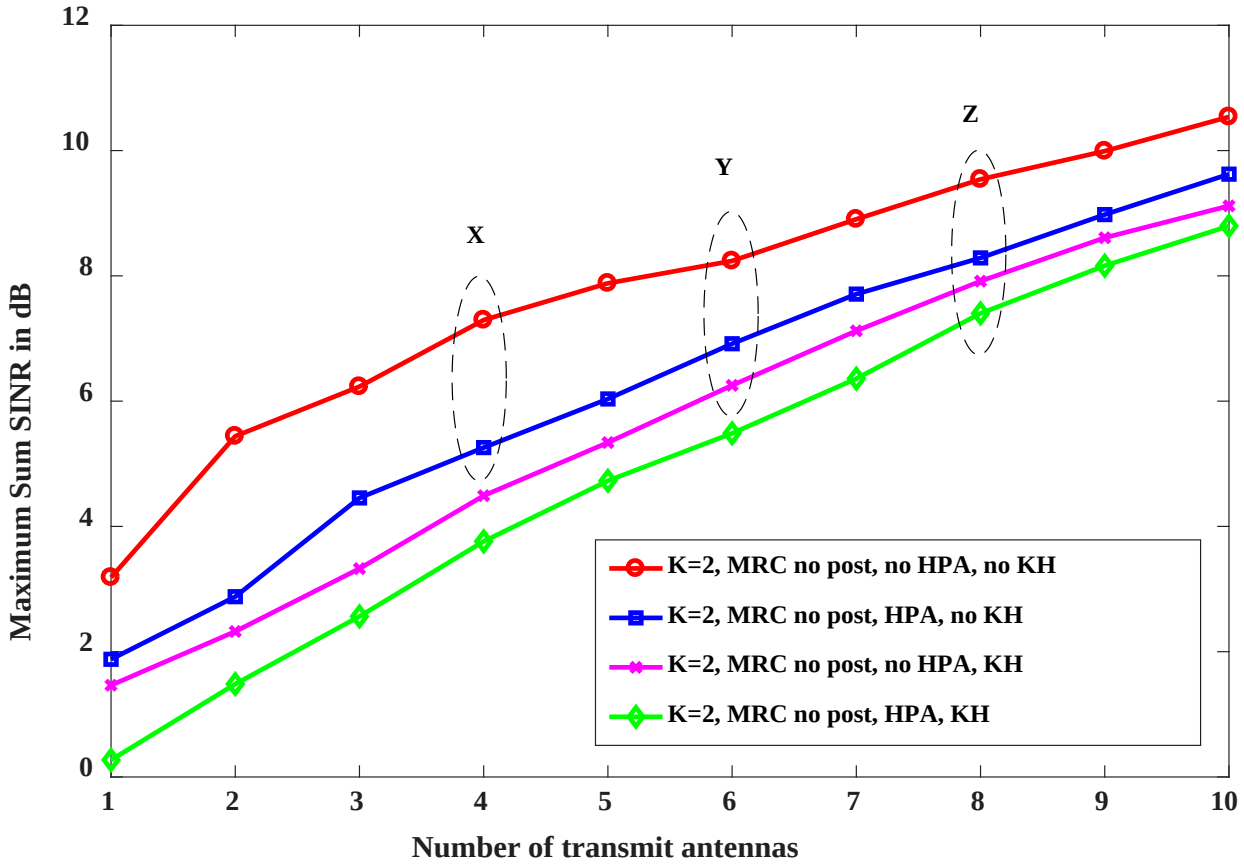

Figure 8. MIMO System Channel Models with No MRC Post Processing for $K = 2$

The encircling denoted by *G* in Figure 9 emphasizes a similar observation for $K = 3$ users. As can be seen, even if the number of users is increased from $K = 2$ to $K = 3$, the sum of the SINR performance is increased. This implies that the DFT-based BF precoding and the MRC post processing can enhance the overall system performance.

Next, we observe that the sum of $SINR_{k,DFT}$ for the MIMO system channel model with KH channels and no HPAs is approximately 2 dB lower than the sum of $SINR_{k,DFT}$ for the system model with no KH channels and no HPAs. It is also less than 1 dB below the sum of $SINR_{k,DFT}$ for the system model with HPAs and no KH channels. The encircling denoted by *Y* in Figure 8 supports this observation for $K = 2$ users. The encircling denoted by *H* in Figure 9 observes the same for $K = 3$ users.

The encircling for *Z* in Figure 8, for $K = 2$ users and the encircling for *I* in Figure 9 for $K = 3$ users both show that the sum of $SINR_{k,DFT}$ for the system model with KH channels and with HPAs is approximately 2–3 dB lower than the sum of $SINR_{k,DFT}$ for the system model with no KH channels and no HPAs, almost 1 dB below the sum of $SINR_{k,DFT}$ for the system model with HPAs and no KH channels, and approximately 0.5 dB below the sum of $SINR_{k,DFT}$ for the system model with KH channels and no HPAs.

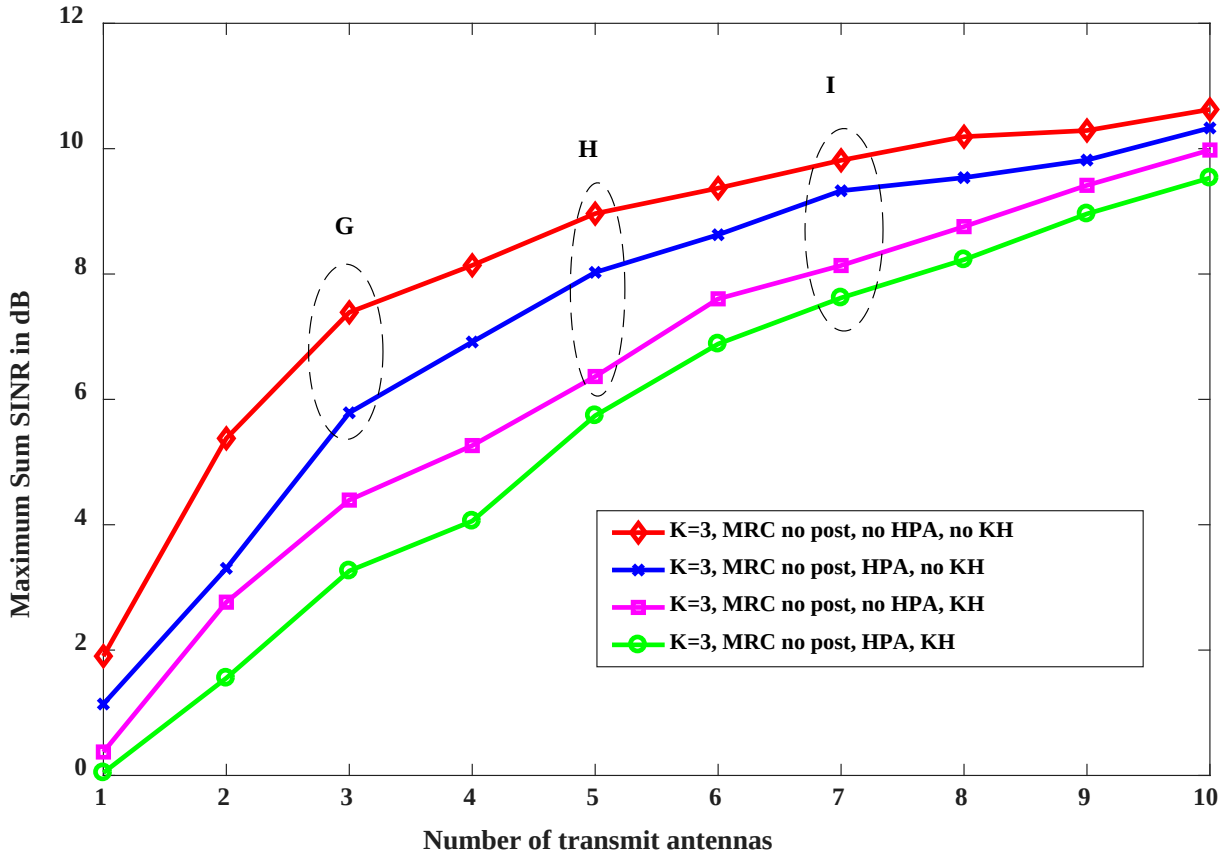

Figure 9. MIMO System Channel Models with No MRC Post Processing for $K = 3$

Next, we use the algorithm in Table I, to perform our simulation. We assume the SINR threshold for user 1 to be 3 dB and for user 2 to be 5 dB when we have $K = 2$ users. When we have $K = 3$ users, we assume the SINR thresholds as 3 dB, 5 dB, and 7 dB, respectively. In Figure 10, we plot individual SINRs for $K = 2$ users from the best combination of optimum weight vectors obtained from the algorithm in Table I and make observations on how many transmit antennas are required such that user SINRs simultaneously satisfy the constraints in Equation (33). In Figure 10, we plot for the MIMO system model, no MRC, no HPA, with KH and with no KH for $K = 2$. As shown, the encirclings denoted by *a*, *b*, *c*, *d*, and *e* clearly show that for $N_t > 5$, user 1 SINR and user 2 SINR simultaneously satisfy the constraints in Equation (33), when the MIMO system model has no HPA and no KH. The encirclings for *f* and *g* shows that when the MIMO system model has no HPA but has a KH channel, the number of transmit antennas supporting SINR constraints in Equation (33) is $N_t > 8$.

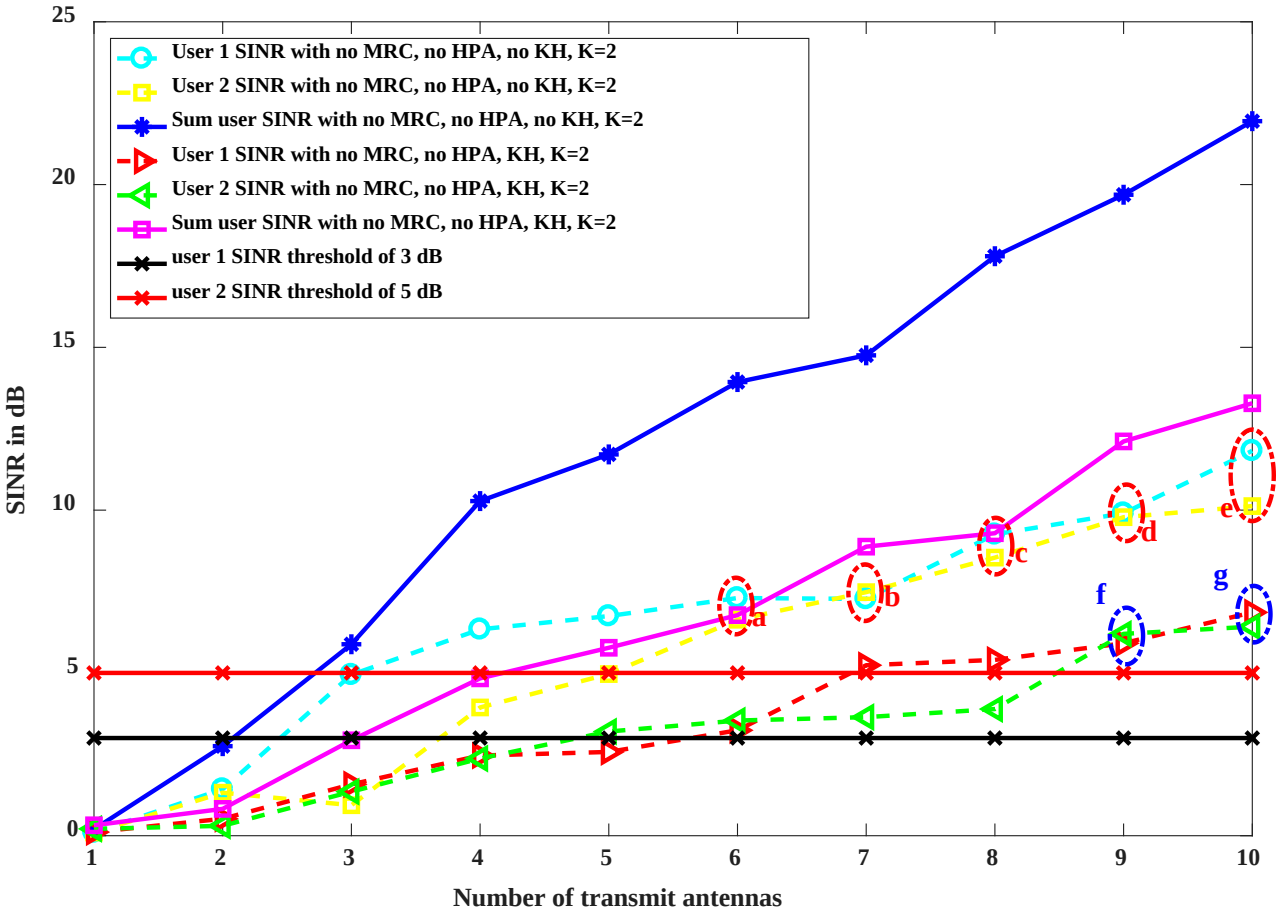

Figure 10. Individual SINR Meeting User Demand SINR for System Model with No MRC Post Processing, No HPA, with KH, and with No KH for $K = 2$

In Figure 11, the encirclings for *h* and *i* denote that for the MIMO system model with HPA and no KH, individual SINRs simultaneously satisfy the constraints in (33) when $N_t > 8$. The encircling for *j*, on the other hand, shows that for $N_t > 9$, the individual SINRs can satisfy the user demand threshold simultaneously.

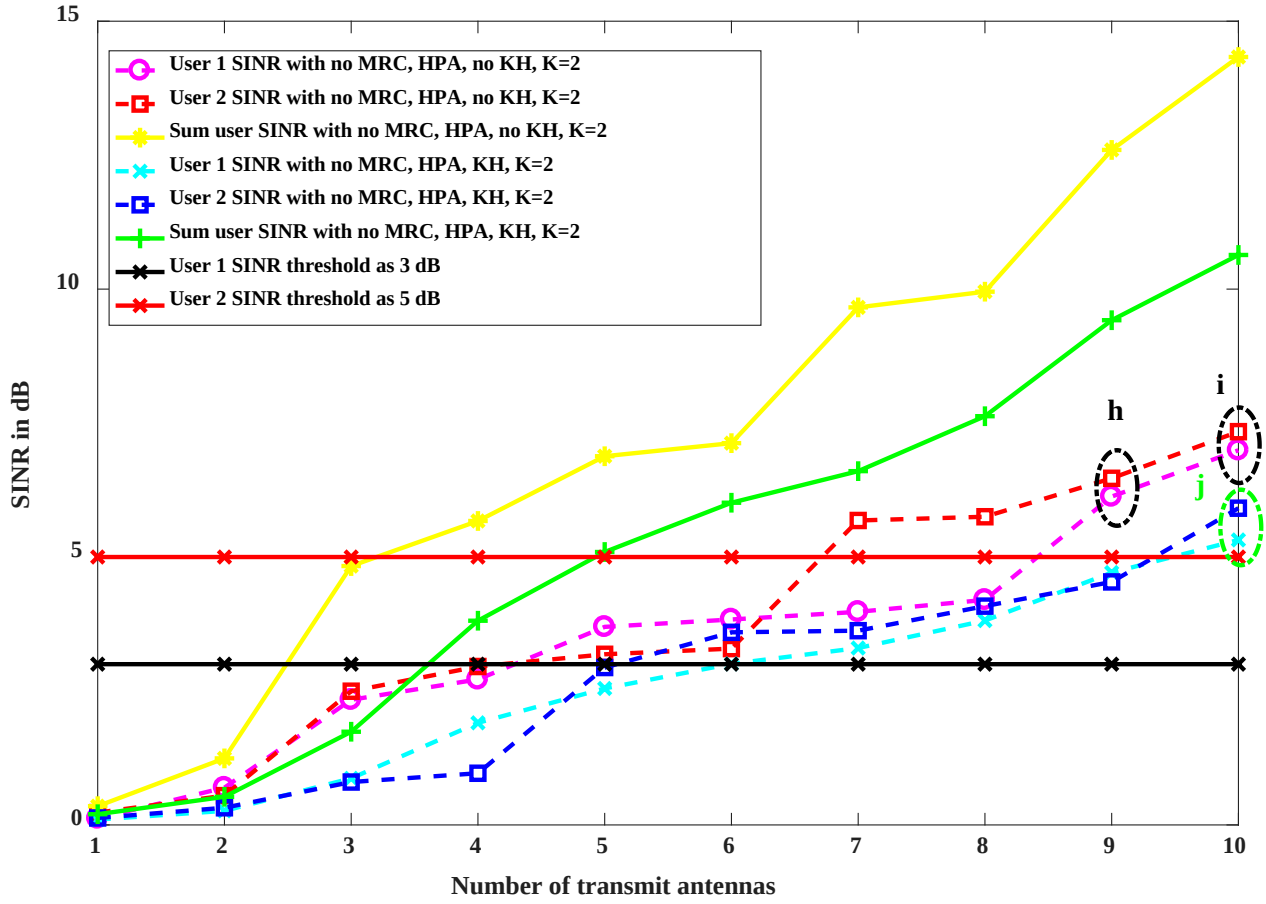

Figure 11. Individual SINR Meeting User Demand SINRs for System Model with No MRC Post Processing, with HPA, with KH, and with No KH for *K* = 2

Figures 12 and 13 show similar results for $K = 3$ users. The encirclings for *k*, *l*, and *m* in Figure 12, show that when there are $K = 3$ users, the individual user SINRs satisfy the SINR thresholds of 3 dB, 5 dB, and 7 dB for $K = 3$ users, respectfully, simultaneously, when $N_t > 7$ and the MIMO system model has no HPA and no KH. When the MIMO system model has no HPA but has a KH channel, even when $N_t = 10$, individual SINRs do not satisfy the SINR constraint as in Equation (33), simultaneously.

In Figure 13, we observe that when the MIMO system model has HPA and no KH, the individual user SINRs for K = 3 meet the SINR threshold constraint as in Equation (33), only for $N_t > 9$. Individual user SINRs are not able to satisfy Equation (33) simultaneously when the MIMO system model has channel degradation effects due to both HPA and the KH channel for $N_t \leq 10$.

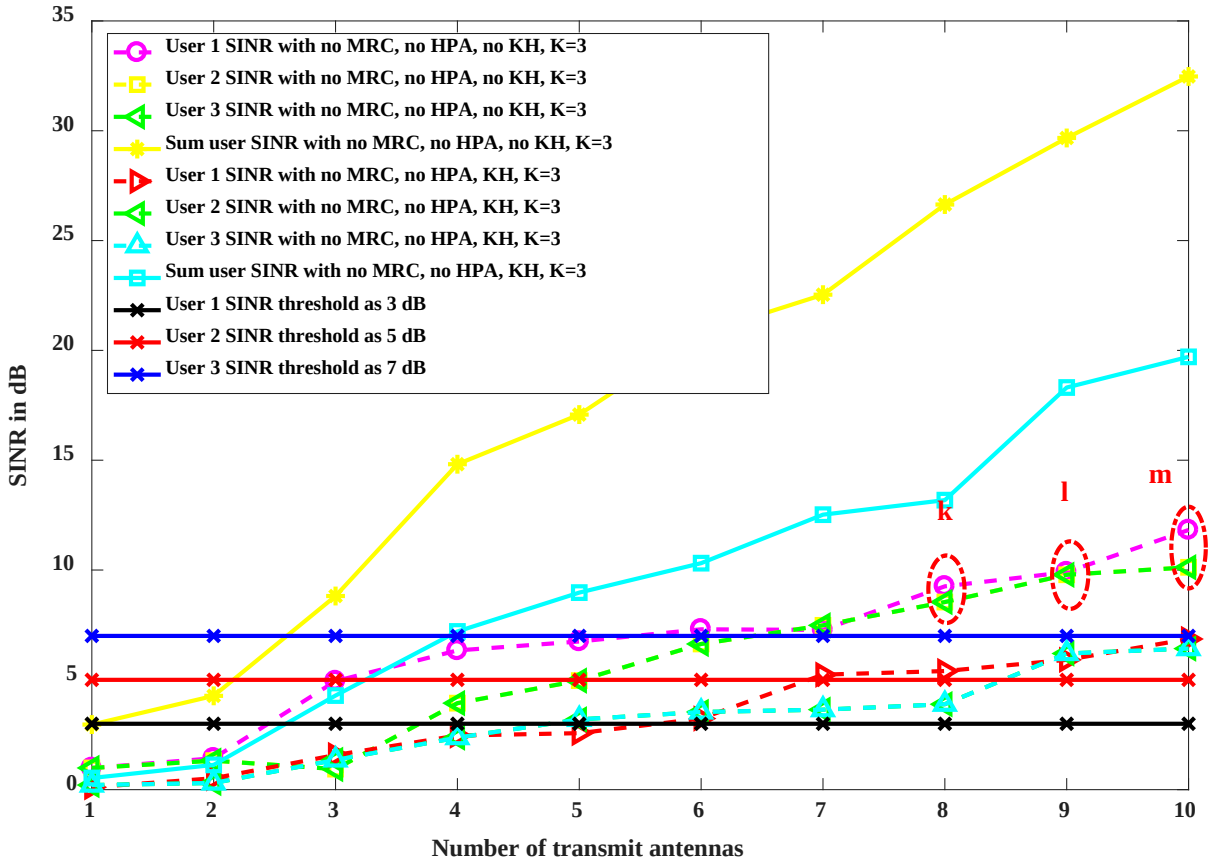

Figure 12. Individual SINR Meeting User Demand SINRs for System Model with No MRC Post Processing, No HPA, with KH, and with No KH for *K* = 3

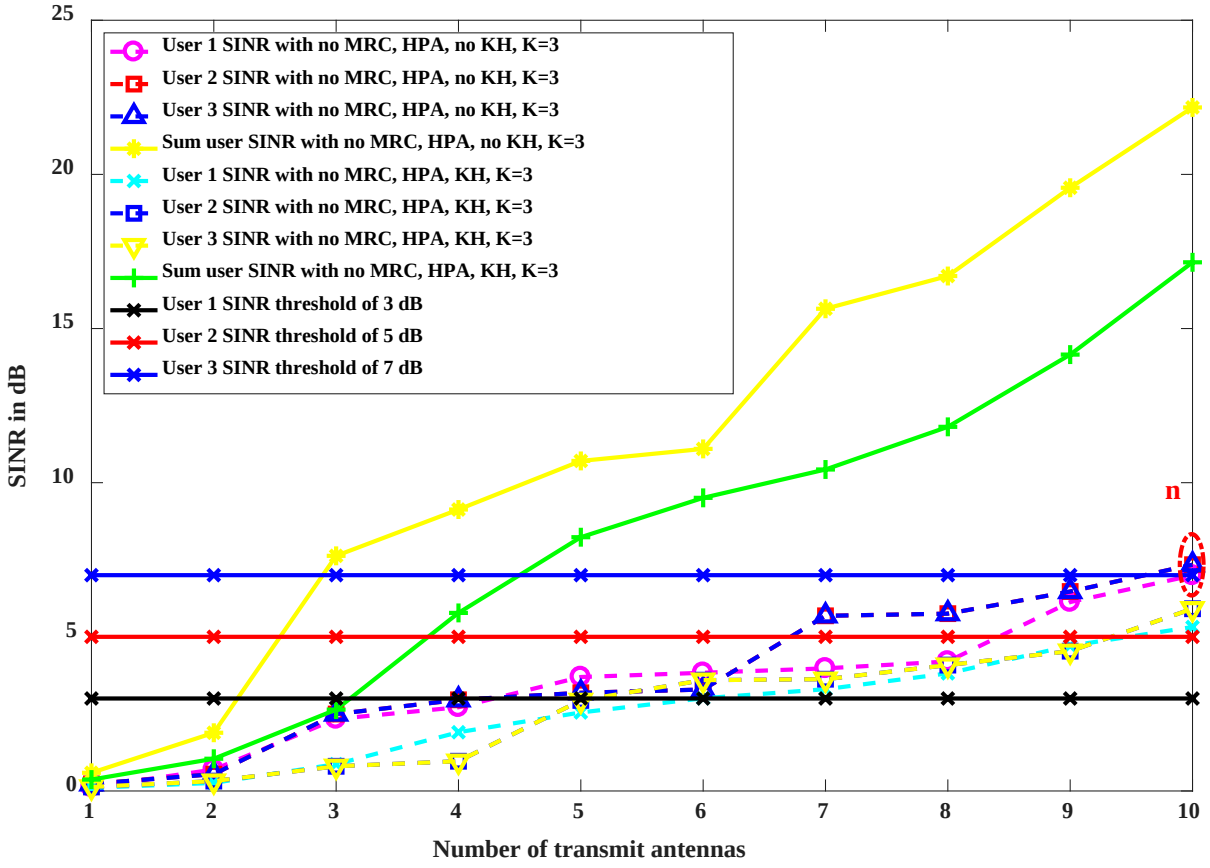

Figure 13. Individual SINR Meeting User Demand SINRs for System Model with No MRC Post Processing, with HPA, with KH, and with No KH for *K*=3

With MRC Post Processing

Here, we focus on the case when MRC post processing is applied to all four system models under discussion.

The sum of $SINR_{k,MRC}$ for the MIMO system channel model with no KH channels and no HPAs, as shown in Figure 14, is approximately 1–2 dB higher than the sum of $SINR_{k,MRC}$ for the system model with HPAs and no KH channels. The encircling denoted by *P* in Figure 14 shows this result clearly, when there are $K = 2$ number of users. In Figure 15, the encircling for *D* supports our above observation for $K = 3$ number of users.

The encircling for *Q* in Figure 14 for $K = 2$ and the encircling for *E* in Figure 15 for $K = 3$ shows that the sum of $SINR_{k,MRC}$ for the system model with KH and no HPAs is approximately 2 dB lower than the sum of $SINR_{k,MRC}$ observed for the system with no KH and no HPAs. Also, it is approximately 1 dB lower than the sum of $SINR_{k,MRC}$ when the model has HPAs but no KH channels.

The encircling for *R* in Figure 14 when there are $K = 2$ number of users, clearly shows that the sum of $SINR_{k,MRC}$ for the system with KH channels and HPAs is approximately 2–3 dB lower than that of the system with no HPAs and no KH channels. Similar results are achieved for $K = 3$ number of users and are denoted by the encircling for *F* in Figure 15. It can also be seen from Figures 14 and 15 that the sum of $SINR_{k,MRC}$ for the system with KH channels and HPAs is approximately 0.5 dB lower than that of the system with KH channels and no HPAs, and 1–2 dB lower than that of the system with HPAs and no KH channels. It is also clearly shown in Figures 8, 9, 14, and 15 that the MRC post processing increases the sum SINR when KH channels are not included. In the presence of KH channels, the performance of the system with the MRC post processing remains the same as under no post processing. This probably occurs because of the highly correlated, and low-ranked KH channel matrix. It has also been observed that the DFT-based BF precoding and the MRC post processing enhances the overall system performance, even for $K > 2$ users. This implies that six users can be supported by the proposed satellite BF with $K = 3$ and two RHC and LHC polarizations.

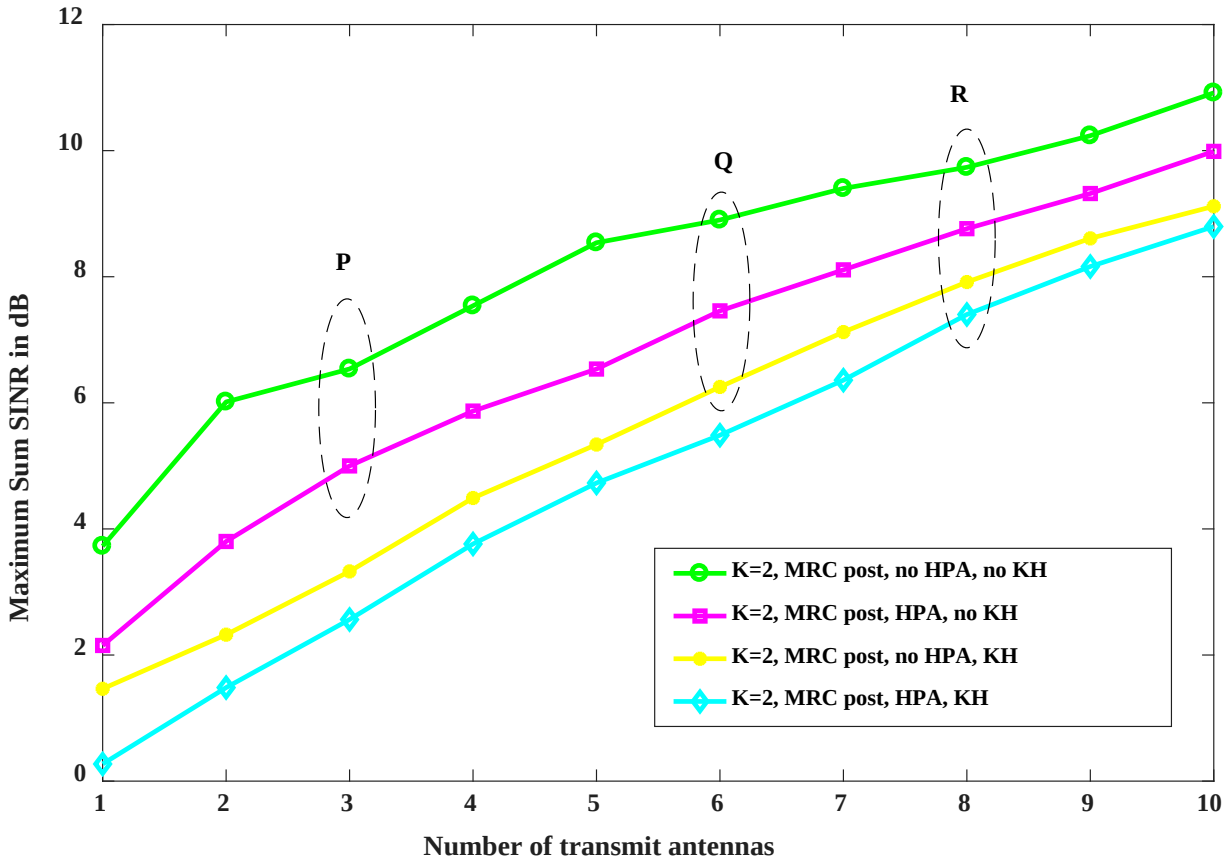

Figure 14. MIMO System Channel Models with MRC Post Processing for *K* = 2

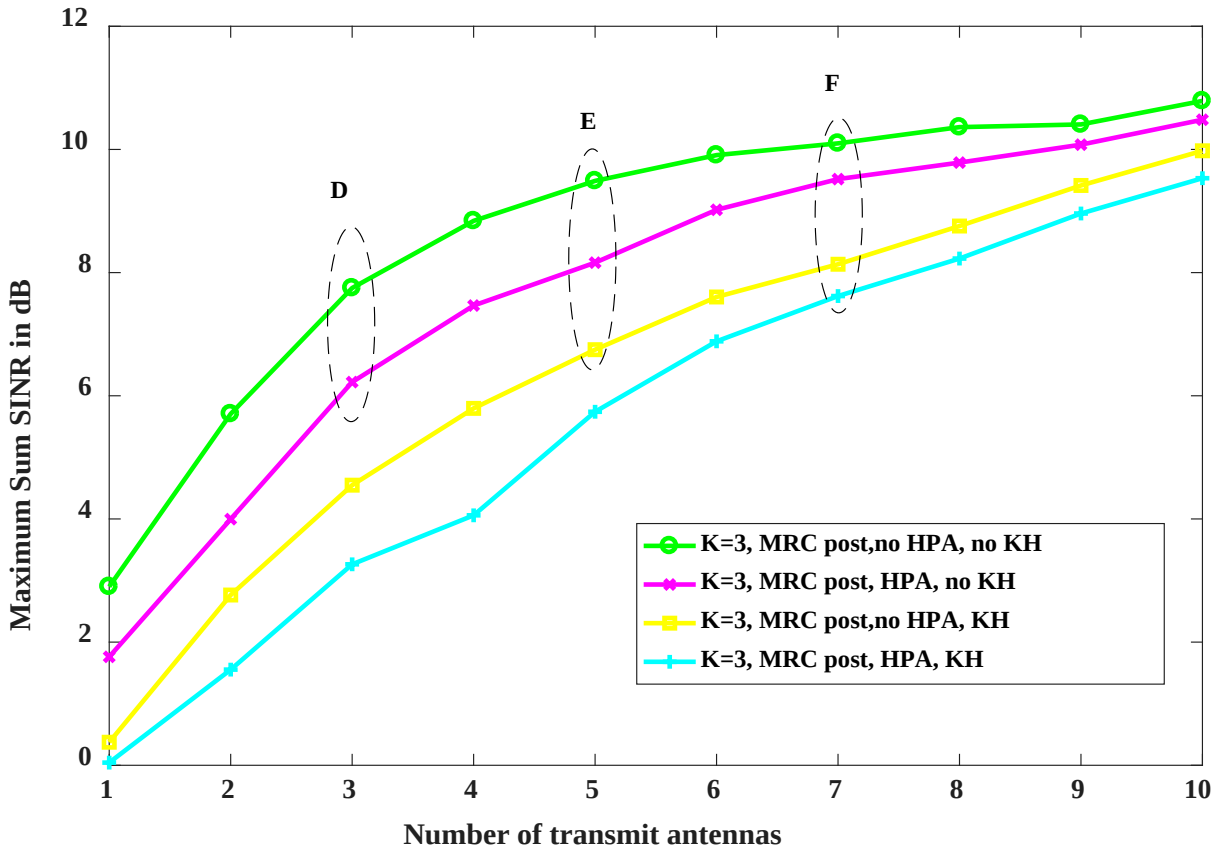

Figure 15. MIMO System Channel Models with MRC Post Processing for *K* = 3

In Figures 16 and 17, the individual user SINR that gives us the maximum sum SINR has been plotted with no MRC post processing and with MRC post processing for $K > 2$. Results show that individual SINRs increase with the number of transmit antennas, and users are also able to reach their target SINR. Similar results follow when we have $K = 2$ users.

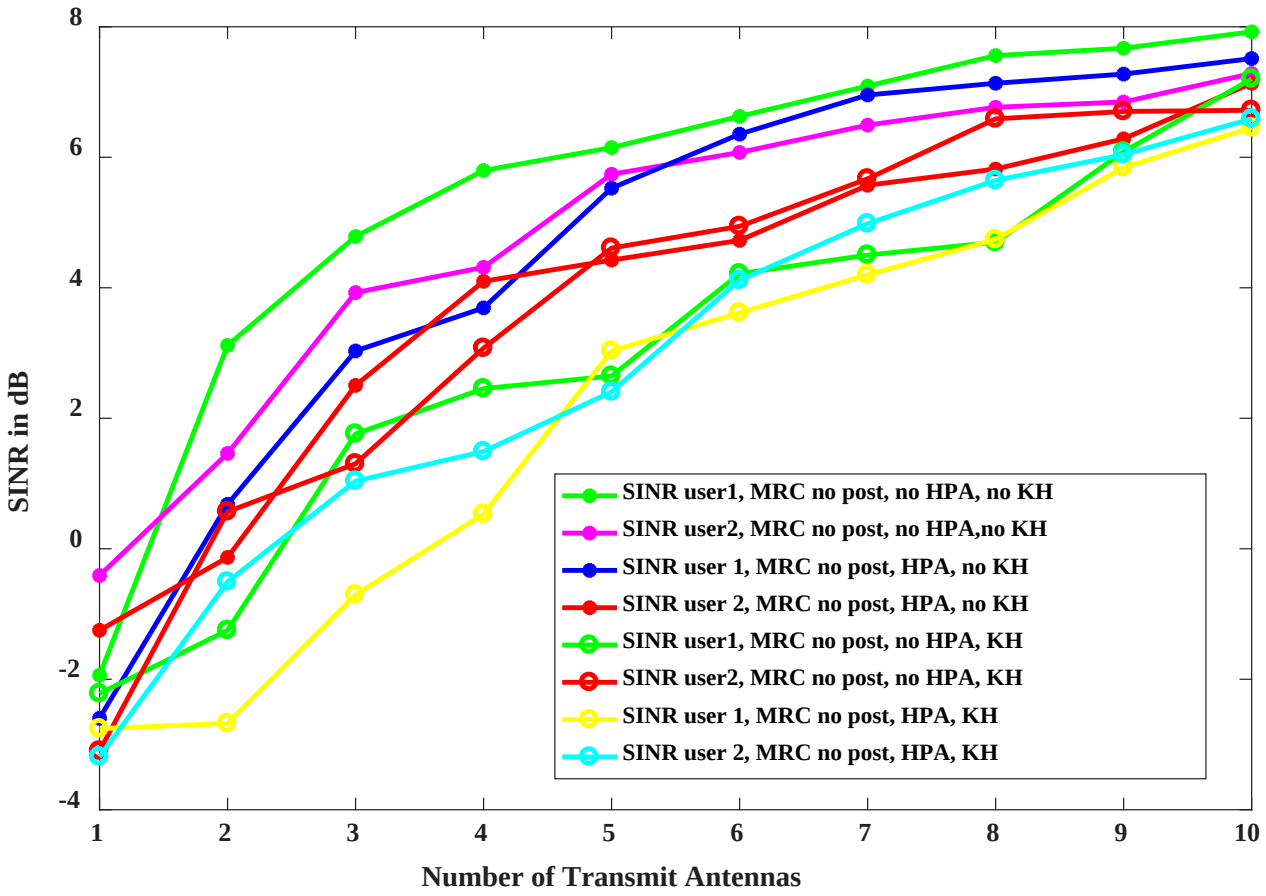

Figure 16. User Specific SINR for MIMO System Channel Models with No MRC Post Processing for $K = 3$

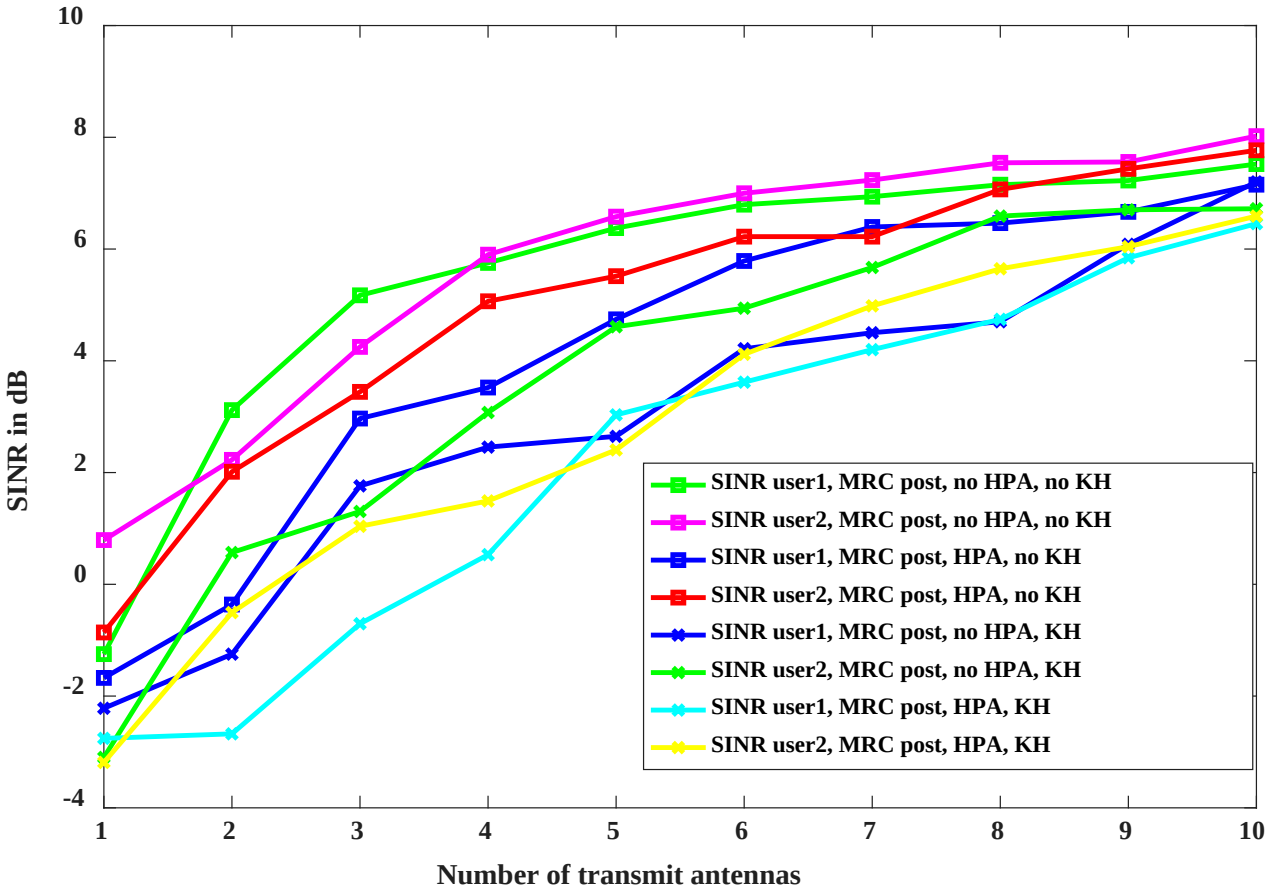

Figure 17. User Specific SINR for MIMO System Channel Models with MRC Post Processing for $K = 3$

Next, we plot individual SINRs for the best combination of optimum weight vectors that achieve the objective in Equation (34). In Figure 18, encirclings for *o*, *p*, *q*, *r*, *s*, and *t* show that, when MRC post processing is applied to the MIMO system model with no HPA and no KH and also with no HPA and with KH, individual SINRs as obtained from the algorithm in Table I satisfy the SINR threshold constraints for $K = 2$ users as in Equation (34), for $N_t > 4$ transmit antennas.

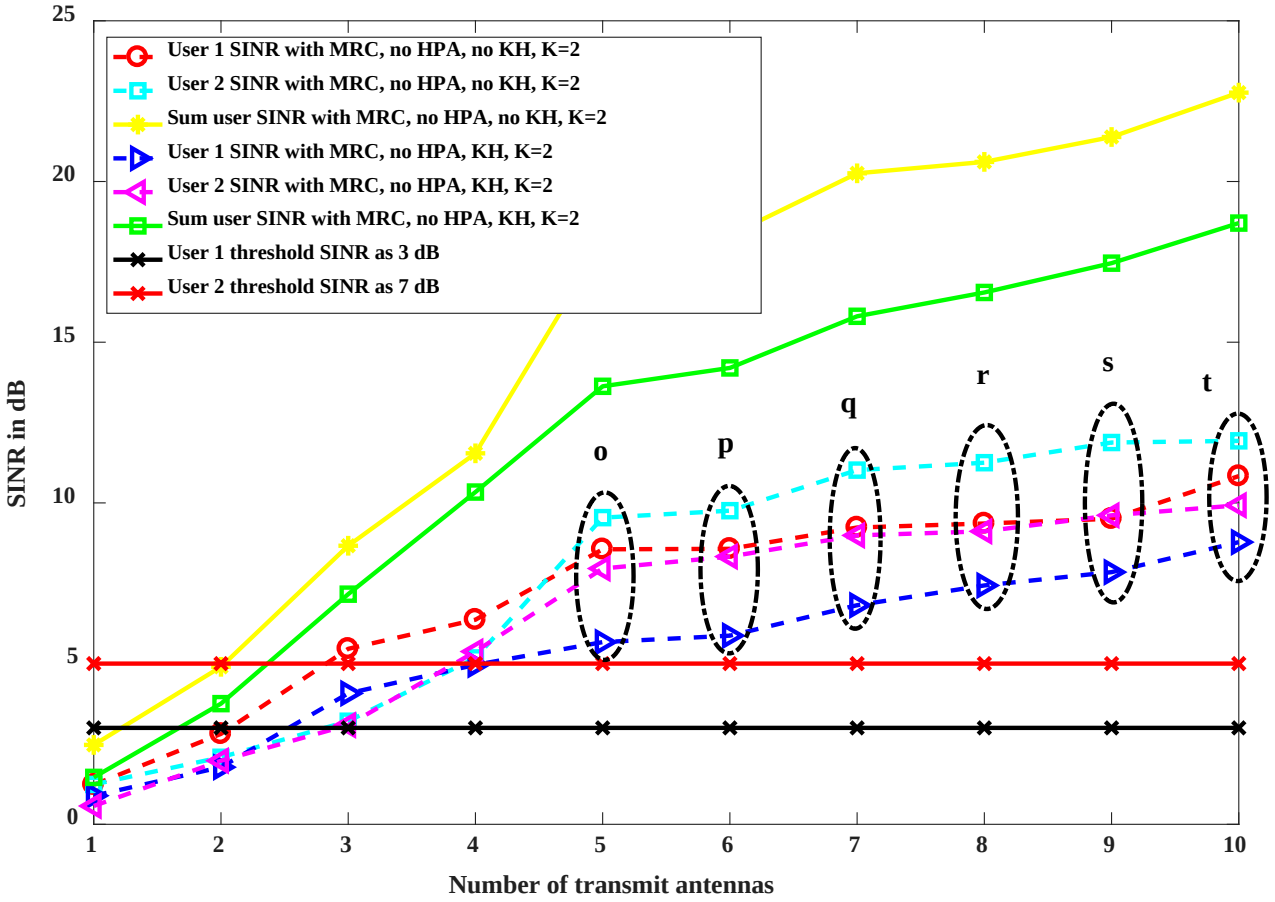

Figure 18. Individual SINR Meeting User Demand SINR for System Model with MRC Post Processing, No HPA, with KH, and with No KH for *K* = 2

In Figure 19, the encirclings for *i*, *ii*, *iii*, *iv*, *v*, and *vi* denote that for $K = 2$ users, when we have an MIMO system model with HPA and no KH, individual user SINRs obtained from the algorithm in Table I satisfy the SINR threshold constraint in Equation (34) for $N_t > 4$. The encircling for *vi* also indicates that when the MIMO system model with HPA and with a KH channel is considered, the individual SINRs satisfy the constraint for $N_t > 9$.

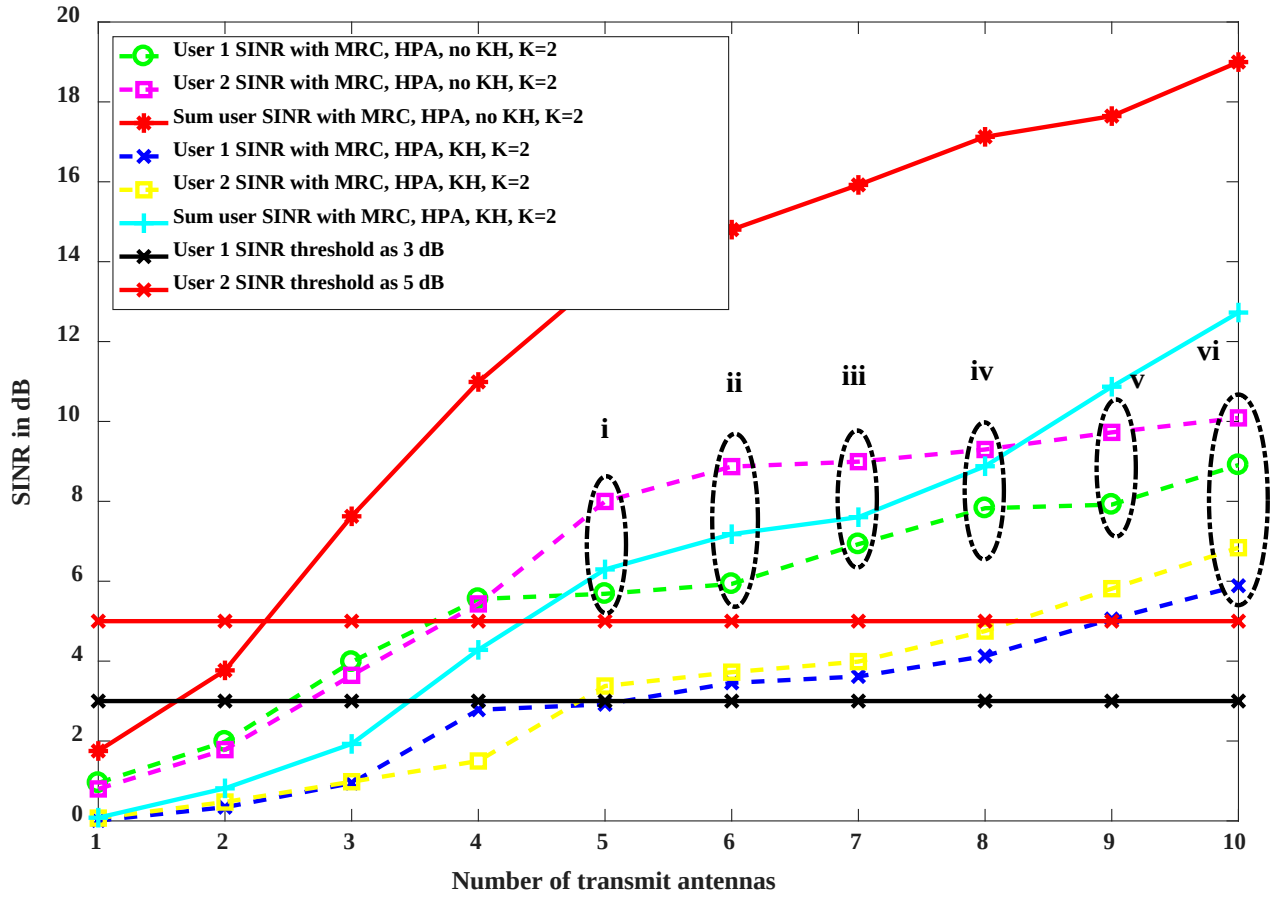

Figure 19. Individual SINR Meeting User Demand SINRs for System Model with MRC Post Processing, with HPA, with KH, and with No KH for *K* = 2

In Figures 20 and 21, we plot the same as above for $K = 3$ users. The encirclings for *w*, *x*, and *y* in Figure 20 denote that for both the MIMO system models with no HPA and no KH, as well as with no HPA and with KH, the individual SINRs obtained using the algorithm in Table I simultaneously exceeds the SINR thresholds of 3 dB, 5 dB, and 7 dB for $K = 3$ users, for $N_t > 7$.

In Figure 21, the encirclings for *vii*, *ix*, and *x* show that for $K = 3$ users, individual SINRs meet the SINR threshold constraint in Equation (30) for $N_t > 7$, when the MIMO system model has HPA but no KH channel. It can also be seen that for the MIMO system model with HPA and with KH, the individual SINRs does not satisfy the SINR constraint for $N_t \leq 10$.

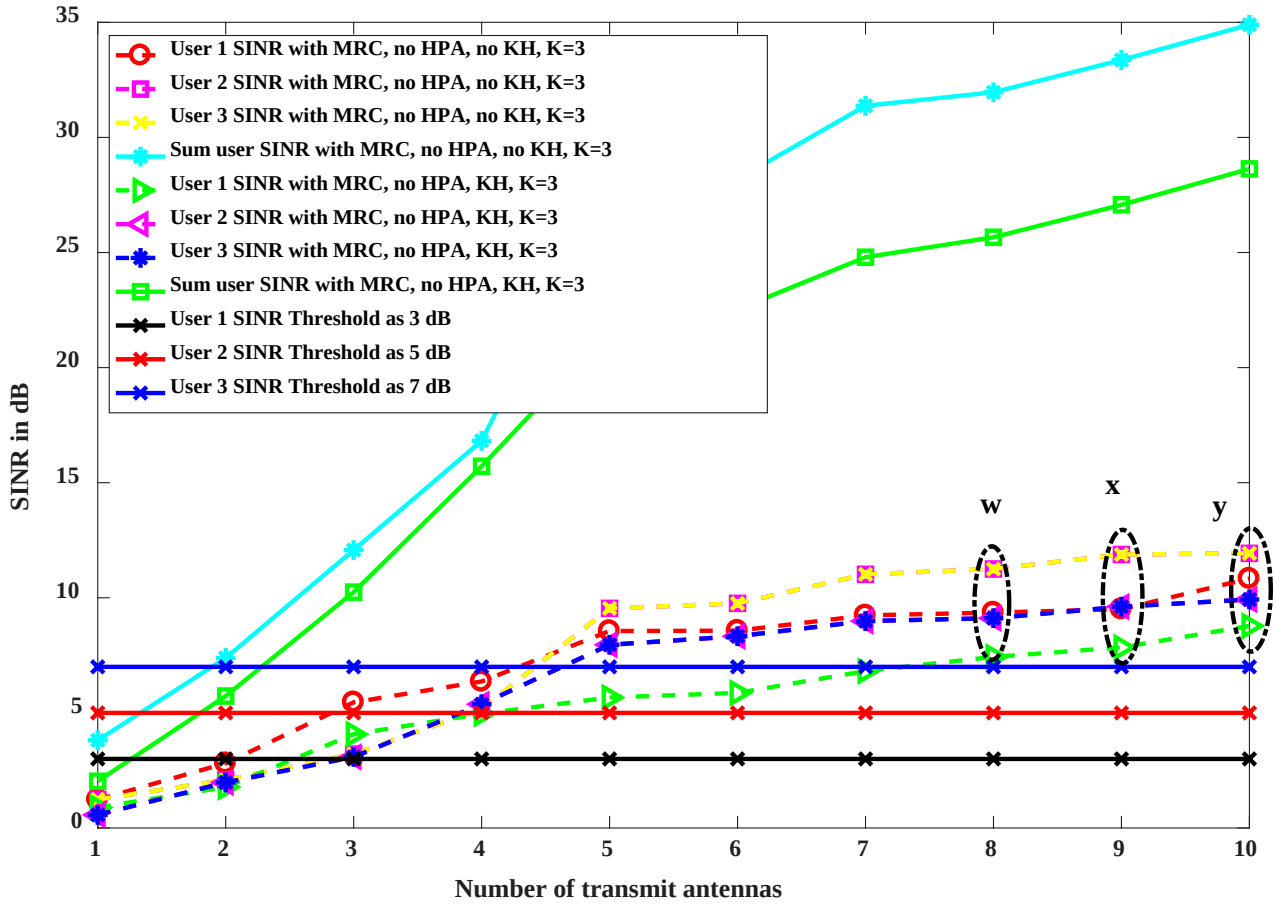

Figure 20. Individual SINR Meeting User Demand SINRs for System Model with MRC Post Processing, with No HPA, with KH, and with No KH for *K* = 3

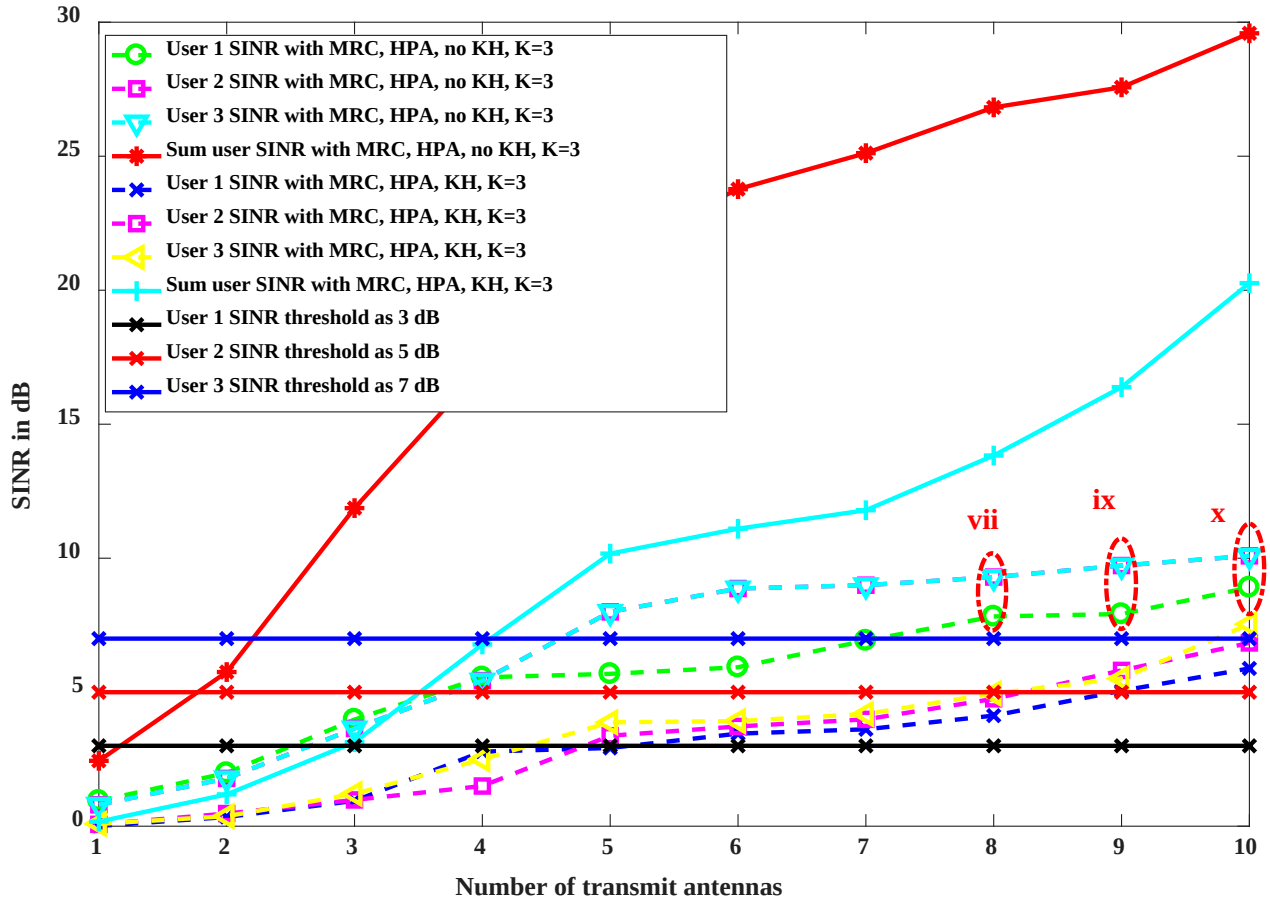

Figure 21. Individual SINR Meeting User Demand SINRs for System Model with MRC Post Processing, with HPA, with KH, and with No KH for $K = 3$

6.0 CONCLUSIONS

Our results in this report clearly indicate the feasibility of satellite digital beamforming with the proposed objectives 1 and 2 in Equations (11) and (12), respectively. In other words, with our proposed method, satellite digital BF is possible to meet the user-specific individual SINR or data rate when the favorable channel propagation condition is met. Our simulation results also show that when channel degradation exists due to HPA and KH channel effects, the user-specific SINR can also be achieved, but this depends on certain conditions like the number of transmit antennas, the number of users, and if the channel is affected by both KH and HPA, or either one. Also, we studied an optimum precoding BF vector combination maximizing the sum of SINRs at the ground/air users by using column vector combinations from a DFT matrix under HPA nonlinearity and keyhole channel environments for $K \geq 2$ users. We made observations that MRC post processing improves the sum SINRs in most cases. But we also observed that under KH channel environments, the MRC

post processing does not improve the received signal quality. In conclusion, 2*K* number of BF user signals can be supported simultaneously with BF and two RHC and LHC polarizations. One drawback of the proposed DFT-based precoding vector method is the feedback requirement that the *K* number of users on the ground/air must report their SINRs to a satellite onboard processor during the training period before transmitting a high volume of data via their return link so that the system controller can determine which weight vector combination maximizes the overall sum SINR. However, this requirement is manageable, because the receiver can send only a one-bit feedback.

REFERENCES

[1] Z. Xiang, M. Tao, and X. Wang, "Massive MIMO Multicasting in Noncooperative Cellular Networks," *IEEE Journal on Selected Areas in Communications*, vol. **32**, no. 6, June 2014.

[2] H. Q. Ngo, E. Larsson, and T. Marzetta, "Energy and Spectral Efficiency of Very Large Multiuser MIMO Systems," *IEEE Transactions on Wireless Communications*, vol. **61**, no. 4, pp. 1436–1449, April 2013.

[3] M. Schubert and H. Boche, "Solution of the Multiuser Downlink Beamforming Problem with Individual SINR Constraints," *IEEE Transactions on Vehicular Technology*, vol. **53**, no. 1, pp. 18–28, 2004.

[4] D. Yang, L.-L. Yang, and L. Hanzo, "DFT-Based Beamforming Weight-Vector Codebook Design for Spatially Correlated Channels in the Unitary Precoding Aided Multiuser Downlink," *2010 IEEE International Conference on Communications*, Cape Town, South Africa, 2010.

[5] V. Joroughi, M. Vázquez, and Ana I. Pérez-Neira, "Generalized Multicast Multibeam Precoding for Satellite Communications," *IEEE Transactions on Wireless Communications*, vol. **16**, no. 2, pp. 952-966, February 2017.

[6] D. Spano, M. Alodeh, S. Chatzinotas, and B. Ottersten, "Symbol-Level Precoding for the Nonlinear Multiuser MISO Downlink Channel," *IEEE Transactions on Signal Processing*, vol. **66**, no. 5, pp. 1331-1345, 1 March 2018.

[7] R. Piazza, M. Shankar, and B. Ottersten "Data Predistortion for Multicarrier Satellite Channels Based on Direct Learning," *IEEE Transactions on Signal Processing*, vol. **62**, no. 22, pp. 5868-5880, 15 November 2014.

[8] A. Kalantari, M. Soltanalian, S. Maleki, S. Chatzinotas, and B. Ottersten, "Directional Modulation via Symbol-Level Precoding: A Way to Enhance Security," *IEEE Journal of Selected Topics In Signal Processing*, vol. **10**, no. 8, pp. 1478-1493, December 2016.

[9] M. Alodeh, S. Chatzinotas, and B. Ottersten, "Constructive Multiuser Interference in Symbol Level Precoding for the MISO Downlink Channel," *IEEE Transactions on Signal Processing*, vol. **63**, no. 9, pp. 2239-2252, 1 May 2015.

[10] C. Masouros and G. Zheng, "Exploiting Known Interference as Green Signal Power for Downlink Beamforming Optimization," *IEEE Transactions on Signal Processing*, vol. **63**, no. 14, pp. 3628-3640, 15 July 2015.

[11] D. Chizhik, G. Foschini, M. Gans, and R. Valenzuela, "Keyholes, correlations, and capacities of multielement transmit and receive antennas," *IEEE Transactions on Wireless Communications*, vol. **1**, no. 2, pp. 361-368, 2002.

[12] A. Saleh, "Frequency-Independent and Frequency-Dependent Nonlinear Models of TWT Amplifiers," *IEEE Transactions on Communications*, vol. **29**, no. 11, pp. 1715-1720, 1981.

[13] D. Self, **Power Amplifier Architecture and Negative Feedback,** in Audio Power Amplifier Design Handbook, 5th ed., Focal Press, pp. 26–61, 2009.

[14] J. Qi and S. Aissa, "Analysis and Compensation of Power Amplifier Nonlinearity in MIMO Transmit Diversity Systems," *IEEE Transactions on Vehicular Technology*, vol. **59**, no. 6, pp. 2921-2931, 2010.

LIST OF SYMBOLS, ABBREVIATIONS, AND ACRONYMS

4G	Fourth-generation
5G	Fifth-generation
AFRL	Air Force Research Laboratory
AM/AM	Amplitude-to-amplitude
AM/PM	Amplitude-to-phase
AWGN	Additive white Gaussian noise
BF	Beamforming
BS	Base station
dB	Decibel
dBW	Decibel Watt
DF	Decode-and forward
DFT	Discrete Fourier Transform
FEC	Forward Error-correction Coding Geostationary
GEO	Earth Orbit
HPA	High Power Amplifier
KH	Keyhole
LHC	Left-hand Circular
MIMO	Multiple-input Multiple-output
MISO	Multiple-input, Single-Output
MRC	Maximal Ratio Combining
RHC	Right-hand Circular
SAT-COM	Satellite Communication
SINR	Signal-to-interference-plus-noise Ratio
TDMA	Time Division Multiple Access

DISTRIBUTION LIST

DTIC/OCP
8725 John J. Kingman Rd, Suite
0944 Ft Belvoir, VA 22060-6218 1 cy

AFRL/RVIL
Kirtland AFB, NM 87117-5776 1 cy

Official Record Copy
AFRL/RVSV/Khanh Pham 1 cy